




**Asymmetry in the Kuramoto model with nonidentical coupling**M. Elaeva *Department of Higher Mathematics, HSE University, Moscow 109028, Russia*E. Blanter  and M. Shnirman *Institute of Earthquake Prediction Theory and Mathematical Geophysics RAS, Moscow 117997, Russia*A. Shapoval *Department of Mathematics and Computer Science, University of Lodz, Lodz 90-238, Poland  
and Cybersecurity Center, Universidad Bernardo O'Higgins, Santiago 8370993, Chile*

(Received 22 October 2022; accepted 26 April 2023; published 5 June 2023)

Synchronization and desynchronization of coupled oscillators appear to be the key property of many physical systems. It is believed that to predict a synchronization (or desynchronization) event, the knowledge on the exact structure of the oscillatory network is required. However, natural sciences often deal with observations where the coupling coefficients are not available. In the present paper we suggest a way to characterize synchronization of two oscillators without the reconstruction of coupling. Our method is based on the Kuramoto chain with three oscillators with constant but nonidentical coupling. We characterize coupling in this chain by two parameters: the coupling strength  $s$  and disparity  $\sigma$ . We give an analytical expression of the boundary  $s_{\max}$  of synchronization occurred when  $s > s_{\max}$ . We propose asymmetry  $A$  of the generalized order parameter induced by the coupling disparity as a new characteristic of the synchronization between two oscillators. For the chain model with three oscillators we present the self-consistent inverse problem. We explore scaling properties of the asymmetry  $A$  constructed for the inverse problem. We demonstrate that the asymmetry  $A$  in the chain model is maximal when the coupling strength in the model reaches the boundary of synchronization  $s_{\max}$ . We suggest that the asymmetry  $A$  may be derived from the phase difference of any two oscillators if one pretends that they are edges of an abstract chain with three oscillators. Performing such a derivation with the general three-oscillator Kuramoto model, we show that the crossover from the chain to general network of oscillators keeps the interrelation between the asymmetry  $A$  and synchronization. Finally, we apply the asymmetry  $A$  to describe synchronization of the solar magnetic field proxies and discuss its potential use for the forecast of solar cycle anomalies.

DOI: [10.1103/PhysRevE.107.064201](https://doi.org/10.1103/PhysRevE.107.064201)**I. INTRODUCTION**

Synchronization phenomenon is a notorious subject whose impact increases with the interest to network dynamics and complex systems. Kuramoto model [1] provides a simple way to study synchronization, which explains its popularity and variability of different applications (see reviews in Refs. [2–4]). Apart from classical applications of the Kuramoto models to systems with huge number of oscillators (e.g., in neuroscience [5]), it starts to be used as a universal way to describe synchronization in time series (see, e.g., Refs. [6–9]). Applied problems inspire exploration of “small-world” systems (e.g., Refs. [10,11]). Focusing on the synchronization properties of solar indices, papers [12–16] represented them with simple Kuramoto models with a few oscillators. Although we had in mind an association between Kuramoto oscillators and solar meridional circulation cells [17–19], it seems that different models applied to the same solar data somehow lead to similar results, representing the loss of synchronization during anomalous solar cycles.

The synchronization between the solar polar field and the sunspot activity manifested in the 11-year solar cycle is observed with all solar indices [20]. Related with solar dynamo and successfully represented by the dynamo models [21], this

synchronization contributes to the solar cycle prediction based on the polar field [22,23]. The polar field is one of the most robust precursors of the next solar cycle. We suspect that if the synchronization allows to predict the start and the strength of the next solar cycle then desynchronization may be the origin of the solar cycle anomalies and the prediction errors. In this paper, we present a technique that allows to identify and potentially forecast desynchronization events and apply this method to solar data.

Kuramoto model successfully catches the desynchronization of the Van der Pol oscillators [24,25]. We come to a hypothesis that to represent synchronization in time series, simple Kuramoto models may be applied in an abstract way without a direct physical connection with the original oscillators. If this is right, then the description and even forecasting of the solar cycle anomalies might be possible without the reconstruction of the network, which is hardly doable process [7,9,26,27]. In the present paper, we apply the chain Kuramoto model with three oscillators to represent synchronization in two time series.

Oscillatory networks with attractive-repulsive interactions [28–30] demonstrate interesting complicated behavior such as antiphase synchronization [31,32], chimera [33,34] or solitary states [35]. Although, theoretically the solitary state is

a special form of weak chimeras [36], we are unable to distinguish between them in finite-size observations. The minimal network allowing solitary states contains  $N = 3$  oscillators [37] and the coupling asymmetry may be important to produce chimeras [36]. Summarizing these findings we consider the chain with  $N = 3$  Kuramoto oscillators with two nonequal and possibly nonpositive coupling coefficients to produce a partial synchronization without further distinguishing between chimera and solitary states, which is impossible for  $N = 3$  as well as for the finite practical observation. However, the disparity of coupling appears to play an important role in the determination of the near-synchronization state in time series. In the present paper, we introduce asymmetry of the order parameter based on the coupling disparity. This asymmetry exhibits invariant scaling properties with respect to the coupling strength and reaches the maximum at the boundary between synchronization and a partial synchronization.

The paper is organized as follows: in Sec. II A, we describe models and solar data. For the chain model with three oscillators we introduce the asymmetry of the generalized order parameter. In Sec. II B, we formulate the self-consistent inverse problem for the chain model and show how the reconstructed asymmetry of the order parameter is related to the synchronization. We apply the reconstruction to the general model and show that scaling properties of the asymmetry remain the same as for the chain. Finally, we apply the reconstruction to solar data. In Sec. III, we summarize the main results. We discuss perspectives and possible applications in Sec. IV. To facilitate the reading, mathematical proofs and details of computations are moved to the Appendices.

## II. MATERIALS AND METHODS

We use a simple chain model to introduce the generalized order parameter  $r$  and determine its asymmetry  $A$  produced by the disparity of coupling coefficients. Then we describe the self-consistent inverse problem used to study properties of the reconstructed asymmetry  $\hat{A}$  and its connection with the coherence of two oscillators. We repeat the inversion procedure but apply it to the model with all-to-all coupling, to see how the network affects the reconstructed asymmetry. Finally, we repeat the same inverse procedure in the third time applying it to the solar proxies, to connect the reconstructed asymmetry with the eventual desynchronization of two solar indices.

### A. Models

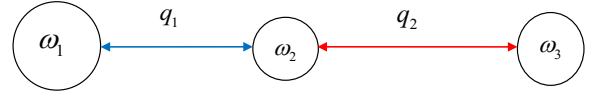
In this paper we use two models with three Kuramoto oscillators coupled as a chain (*chain model*) or all-to-all (*general model*) network, sketched at Fig. 1.

#### 1. Chain model

We take three Kuramoto oscillators with nonequal natural frequencies  $\omega_i$ , coupled in a chain with two nonequal coupling coefficients  $q_1$  and  $q_2$  (Fig. 1, top). Their phases  $\theta_i$  satisfy the classical Kuramoto equation [1,2]

$$\dot{\theta}_i(t) = \omega_i + \sum_{j=1}^3 \kappa_{ij} \sin[\theta_j(t) - \theta_i(t)], \quad i = 1, 2, 3, \quad (1)$$

#### CHAIN MODEL



#### GENERAL MODEL

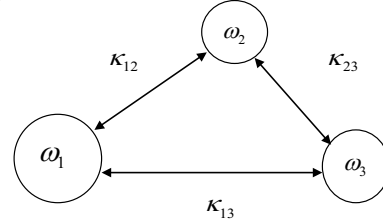


FIG. 1. Schematic representation of three nonidentical Kuramoto oscillators coupled in a chain (top) and all-to-all (bottom) network.

where  $\kappa_{12} = \kappa_{21} = q_1$ ,  $\kappa_{23} = \kappa_{32} = q_2$ , and  $\kappa_{13} = \kappa_{31} = 0$ . The nonzero coupling coefficients  $q_1$  and  $q_2$  are constant but may be negative as well as positive. Typically, the case of constant natural frequencies  $\omega_i = \text{const}$  is considered, but slowly evolving functions  $\omega_i(t)$  are also allowed in this model.

Taking the sum of equations in Eq. (1) we get that the mean frequency  $\Omega$  is equal to the average natural frequency if  $\kappa_{ij} = \kappa_{ji}$ :

$$\Omega = \frac{\dot{\theta}_1 + \dot{\theta}_2 + \dot{\theta}_3}{3} = \frac{\omega_1 + \omega_2 + \omega_3}{3}. \quad (2)$$

Let us denote the symmetrical and antisymmetrical components of the two coupling coefficients  $q_1$  and  $q_2$  as  $k = (q_1 + q_2)/2$  and  $\Delta k = (q_1 - q_2)/2$ , respectively. We define the coupling strength  $s$  and disparity  $-1 < \sigma < 1$  as

$$s = \max(|k|, |\Delta k|), \quad \sigma = \begin{cases} \frac{\Delta k}{k} & \text{if } s = |k|, \\ \frac{k}{\Delta k} & \text{if } s = |\Delta k|. \end{cases} \quad (3)$$

Essentially nonidentical and nonpositive coupling coefficients require generalization of the order parameter. It becomes a weighted sum of local order parameters and eventually loses its symmetry (see, e.g., the asymmetrical order parameter in Kuramoto-Sakaguchi network [38]). We consider the real part of the order parameter as it was done by Schröder *et al.* [39] (see Appendix A for details) and get

$$r = \frac{q_1 \cos(\theta_1 - \theta_2) + q_2 \cos(\theta_2 - \theta_3)}{|q_1| + |q_2|}. \quad (4)$$

We note that  $r$  is defined for positive and negative values of coupling  $q_1$  and  $q_2$ , attaining values between  $-1$  and  $1$ . If the coupling coefficients are identical,  $q_1 = q_2 = K$  and  $\sigma = 0$ , then  $r$  corresponds to the frustration  $F$  [29,40,41] as  $r = F - 1$ . Positive identical coupling coefficients  $q_i = K > 0$  provide the positive values of  $r = r_{\text{uni}}$  [39].

Let us express the order parameter (4) through the disparity  $\sigma$  and two phase differences  $\alpha = (\theta_1 - \theta_3)/2$  and  $\beta = (\theta_1 + \theta_3)/2 - \theta_2$ :

$$r = \begin{cases} \frac{1+\sigma}{2} \cos(\alpha + \beta) + \frac{1-\sigma}{2} \cos(\alpha - \beta), & s = |k|, \\ \frac{1+\sigma}{2} \cos(\alpha + \beta) - \frac{1-\sigma}{2} \cos(\alpha - \beta), & s = |\Delta k|. \end{cases} \quad (5)$$

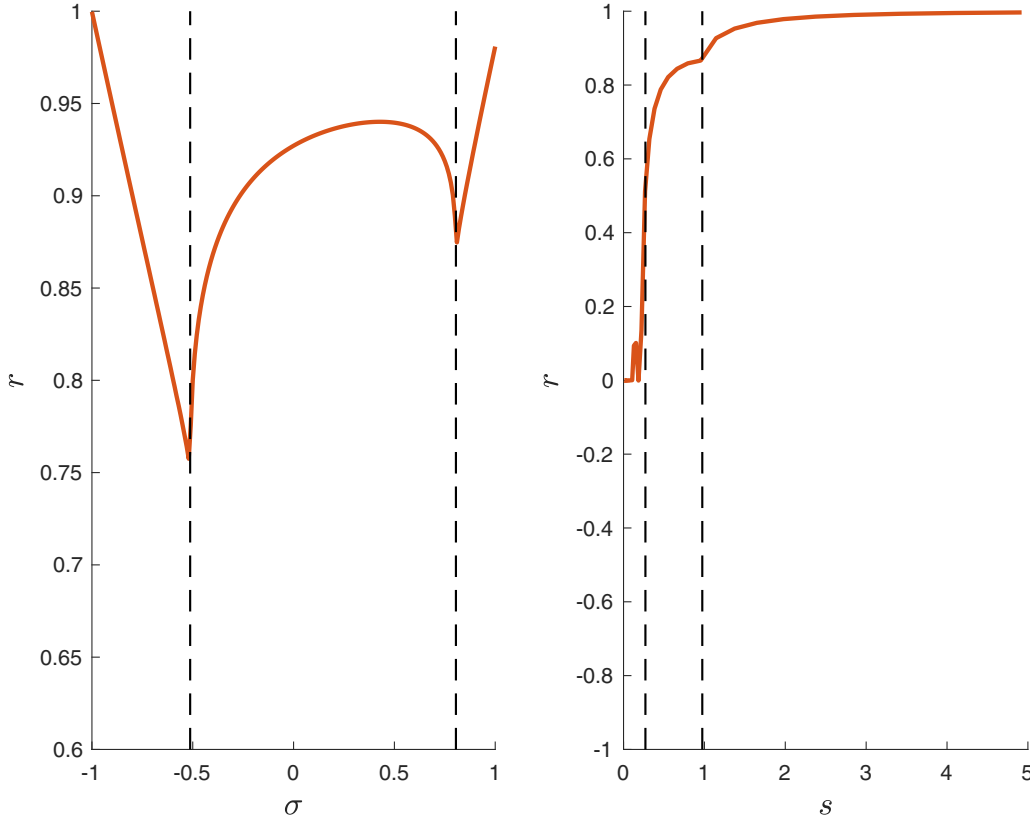


FIG. 2. The order parameter  $r$  as the function of the disparity  $\sigma$  (left) and coupling strength  $s$  (right) in the chain model. Vertical dashed lines indicate two phase transitions corresponding to the boundaries of the partial synchronization  $\sigma^+$  and  $\sigma^-$  (left),  $s_{\min}$  and  $s_{\max}$  (right) (see Appendix A). The natural frequencies are the same as in Fig. 10 of Appendix A. The free coupling parameters are  $s = |\Delta k| = 1$  (left panel),  $\sigma = 0.8$  (right panel).

We note that although  $r$  given by Eq. (5), like the classical order parameter, does not include the coupling strength  $s$  explicitly, it does depend on  $s$  through the phase differences  $\alpha$  and  $\beta$ . Figure 2 (right) demonstrates two phase transitions: (i) from the decoherence of three oscillators (*desynchronization*) to two coherent and one drifting oscillators (*partial synchronization*), and (ii) from the partial synchronization to the coherence of all oscillators (*synchronization*). In the case of synchronization the phase differences converge to their limits  $\tilde{\alpha} = \lim_{t \rightarrow \infty} \alpha(t)$  and  $\tilde{\beta} = \lim_{t \rightarrow \infty} \beta(t)$ . Considered modulus  $2\pi$  the stable stationary phase difference  $2\tilde{\alpha} = \lim_{t \rightarrow \infty} (\theta_1 - \theta_3)$  appears to be in a neighborhood of 0 ( $|2\tilde{\alpha}| < \pi/2$ ) when  $s = |k|$ , and in a neighborhood of  $\pi$  ( $|2\tilde{\alpha}| > \pi/2$ ) when  $s = |\Delta k|$  (see Appendix A for details). We note that the phase difference  $|2\tilde{\alpha}| = \pi/2$  cannot be realized for the stable synchronization.

Figure 2 (left) shows that the order parameter  $r$  is asymmetric with respect to  $\sigma = 0$ . We introduce the asymmetry  $A$  of the order parameter as

$$A(\sigma, s) = |r(\sigma, s) - r(-\sigma, s)|. \quad (6)$$

Simple calculations show that for constant natural frequencies and  $\omega_2 \neq \Omega$  the asymmetry  $A$  decays with the coupling strength  $s$  at least as

$$A(\sigma, s) \sim \frac{1}{s^2}, \quad 0 < \sigma < 1 \quad (7)$$

(see Appendix B for the proof).

## 2. General model

As a general model, we consider three Kuramoto oscillators with constant but nonequal natural frequencies  $\omega_i = \text{const}$ ,  $i = 1, 2, 3$  coupled with all-to-all constant couplings  $\kappa_{ij} = \kappa_{ji} = \text{const} \neq 0$ . Their phase evolution is given by the Kuramoto Eq. (1), but there are three nonzero coupling coefficients. The mean frequency satisfies Eq. (2).

## 3. Solar data

We consider proxies of two components of solar magnetic field (toroidal and poloidal) [42], because they are evolving in antiphase but have the same 11-year solar cycle (Fig. 3). As a proxy of the toroidal component we use hemispheric sunspot numbers  $T(t)$  available with daily sampling in Ref. [43] covering the time interval 1874–2020 [44]. As a proxy of the poloidal component we use two data series of yearly sampled polar faculae: Mount Wilson Observatory (MWO) solar faculae count  $P_m(t)$ , calibrated to fit the polar field of Wilcox Solar Observatory, available on the time interval 1906–2012 [45] and Pulkovo Observatory synthetic polar faculae series  $P_p(t)$  available at Ref. [46]. We interpolate the polar faculae data to the daily sampled series  $P(t)$  using cubic splines as we did in our previous work [15].

We process the series and build the solar cycle phases  $\Phi_T(t)$ ,  $\Phi_{P_m}(t)$  and  $\Phi_{P_p}(t)$  by using the Fourier transform with respect to the average solar cycle length of 10.75 years in the

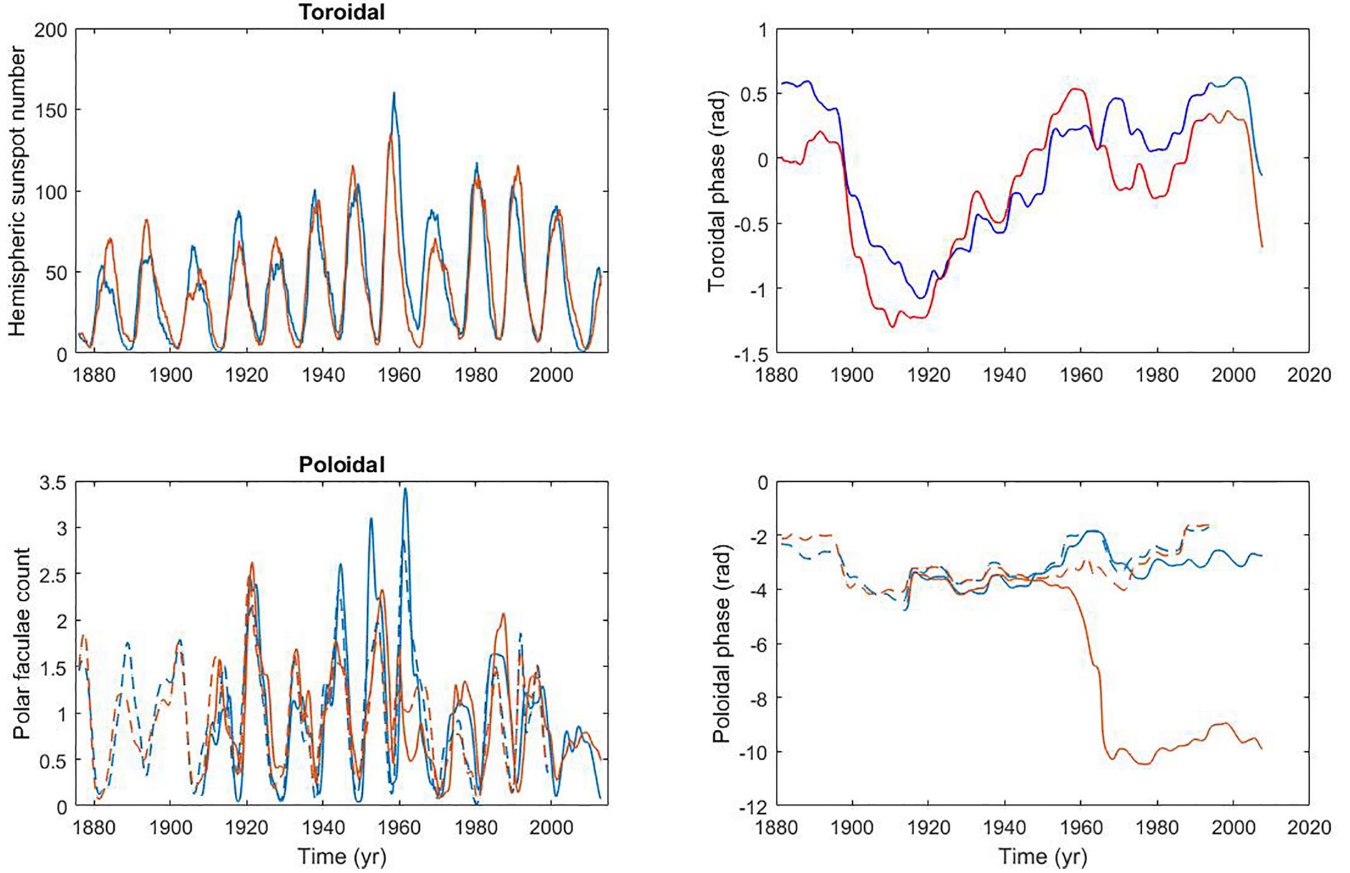


FIG. 3. Observed evolution of the solar data in the northern (blue) and southern (red) hemispheres. Left: 2-year averaged proxies of the toroidal (top) and poloidal (bottom) solar field component; top right: the phase evolution of the toroidal component; bottom right: the phase evolution of the poloidal component for MWO/WSO (solid) and Pulkovo (dashed) data. Desynchronization event of 1960 in the southern hemisphere exists only on the MWO/WSO data (solid red line in the right bottom panel).

same way we did in our previous works [15,16] (see details in Appendix E). The phase of the toroidal component evolves slowly in agreement with regularities of the solar cycle (Fig. 3, top) when the phase of the poloidal component  $\Phi_{pm}$  in the southern hemisphere exhibits a phase slip representing irregularity of the solar cycle in 1960 (Fig. 3, bottom).

### B. Self-consistent reconstruction

In this section we reconstruct the evolution of natural frequencies  $\hat{\omega}_i(t)$  from the observed phase difference  $\alpha(t)$  for given coupling parameters  $\hat{s}$  and  $\hat{\sigma}$ . Let us note, that we apply the reconstruction to two particular oscillators, assuming that they are the edges of a chain with three Kuramoto oscillators. The coupling strength  $\hat{s}$  and disparity  $\hat{\sigma}$  used in the reconstruction are different from the true coupling strength  $s$  and disparity  $\sigma$ , therefore we do not require the reconstructed natural frequencies  $\hat{\omega}_i$  to be equal, or even close, to the true natural frequencies  $\omega_i$ . The reconstruction is called self-consistent when the phase difference  $\hat{\alpha}(t)$  simulated with the chain model with natural frequencies  $\hat{\omega}_i(t)$  and coupling strength  $\hat{s}$  and disparity  $\hat{\sigma}$  appears to be close to the observed phase difference  $\alpha(t)$ . Theoretically, in the case of synchronization we require  $\lim_{t \rightarrow \infty} \alpha(t) = \lim_{t \rightarrow \infty} \hat{\alpha}(t)$ ; however, in practical applications and finite time series, a certain proximity is sufficient (see Appendix C for details).

Solving the self-consistent inverse problem we take into account that the stable stationary solution of the Kuramoto equations for the chain of three oscillators under condition of phase locking determines the phase difference  $\tilde{\alpha} = \lim_{t \rightarrow \infty} \alpha(t)$ :

$$\begin{aligned} |2\tilde{\alpha}| &< \frac{\pi}{2}, & \text{if } s = |k|, \\ |2\tilde{\alpha}| &> \frac{\pi}{2}, & \text{if } s = |\Delta k|. \end{aligned} \quad (8)$$

We perform the self-consistent reconstruction *assuming* that the phase locking is almost reached at each time moment of observations  $t$  and the observed phase difference  $\alpha(t)$  is close to  $\lim_{\tau \rightarrow \infty} \alpha(t + \tau)$ .

#### 1. Application to the chain model

In the chain model we always use the phase difference between two edge oscillators  $\alpha(t) = [\theta_1(t) - \theta_3(t)]/2$ . We solve the self-consistent inverse problem reconstructing the difference between natural frequencies  $\Delta\hat{\omega} = \hat{\omega}_1(t) - \hat{\omega}_3(t)$  for fixed parameters:  $\hat{\omega}_2 = 0$ , coupling disparity  $\hat{\sigma} \neq 0$  and coupling strength  $\hat{s}$ . Performing the reconstruction, we use the following equations obtained from Eq. (1) with  $s = \hat{s}$ ,  $\sigma = \hat{\sigma}$ ,



and  $\omega_2 = \hat{\omega}_2$ :

$$\begin{aligned}\dot{\alpha} &= \Delta\omega - \hat{s}(\sin\alpha \cos\beta - \hat{\sigma} \sin\beta \cos\alpha), \\ \dot{\beta} &= \frac{3}{2}(\Omega - \hat{\omega}_2) - 3\hat{s}(\sin\beta \cos\alpha - \hat{\sigma} \sin\alpha \cos\beta), \quad |2\alpha| < \frac{\pi}{2}, \\ \dot{\alpha} &= \Delta\omega - \hat{s}(\hat{\sigma} \sin\alpha \cos\beta - \sin\beta \cos\alpha), \\ \dot{\beta} &= \frac{3}{2}(\Omega - \hat{\omega}_2) - 3\hat{s}(\hat{\sigma} \sin\beta \cos\alpha - \sin\alpha \cos\beta), \quad |2\alpha| > \frac{\pi}{2}.\end{aligned}$$

Here the phase difference  $\alpha = \alpha(t)$  is known and the phase difference  $\beta = [\theta_1(t) + \theta_3(t)]/2 - \theta_2(t)$  is unknown. The reconstruction is performed in two steps. First, we express the unknown phase difference  $\beta(t) = \hat{\beta}$  through  $\alpha(t)$  from the differential equation with respect to  $\beta$  assuming  $\alpha(t)$  to be a known constant (see Appendix C 1 for details). Second, we substitute  $\hat{\beta}$  to express the difference between natural frequencies  $\Delta\hat{\omega}$  through  $\alpha = \alpha(t)$  under condition of the phase locking ( $\dot{\alpha} = 0$ ):

$$\Delta\hat{\omega} = \begin{cases} \frac{\hat{\sigma}(\Omega - \hat{\omega}_2) + |\hat{s}|(1 - \hat{\sigma}^2) \sin 2\tilde{\alpha} \sqrt{\cos^2 \tilde{\alpha} + \hat{\sigma}^2 \sin^2 \tilde{\alpha} - \frac{(\Omega - \hat{\omega}_2)^2}{4\hat{s}^2}}}{2(\hat{\sigma}^2 \sin^2 \tilde{\alpha} + \cos^2 \tilde{\alpha})}, & |2\alpha| < \frac{\pi}{2}, \\ \frac{\hat{\sigma}(\Omega - \hat{\omega}_2) - |\hat{s}|(1 - \hat{\sigma}^2) \sin 2\tilde{\alpha} \sqrt{\hat{\sigma}^2 \cos^2 \tilde{\alpha} + \sin^2 \tilde{\alpha} - \frac{(\Omega - \hat{\omega}_2)^2}{4\hat{s}^2}}}{2(\sin^2 \tilde{\alpha} + \hat{\sigma}^2 \cos^2 \tilde{\alpha})}, & |2\alpha| > \frac{\pi}{2}. \end{cases} \quad (9)$$

Natural frequencies are then obtained as

$$\hat{\omega}_1 = \frac{3}{2}\Omega - \frac{\hat{\omega}_2}{2} + \Delta\hat{\omega}, \quad \hat{\omega}_3 = \frac{3}{2}\Omega - \frac{\hat{\omega}_2}{2} - \Delta\hat{\omega}. \quad (10)$$

Although the reconstructed difference between natural frequencies  $\Delta\hat{\omega}$  is not equal to their original difference  $\Delta\omega$  for unknown parameters  $\hat{s} \neq s$ ,  $\hat{\sigma} \neq \sigma$ ,  $\hat{\omega}_2 \neq \omega_2$ , the above procedure under certain conditions correctly reconstructs its sign for the strong coupling  $\hat{s}$  (see Appendix C 3 for details).

We note that Eq. (9) means that in the case of synchronization  $\alpha(t) = \text{const}$ , the reconstructed difference between natural frequencies is also constant:  $\Delta\hat{\omega} = \text{const}$ . The difference between natural frequencies  $\Delta\hat{\omega}$  reconstructed for a fixed disparity  $\hat{\sigma} > 0$  linearly increases with the coupling strength  $\hat{s}$ .

Equation (9) yields that the reconstruction gives  $\Delta\hat{\omega}(\hat{\sigma}) \neq \Delta\hat{\omega}(-\hat{\sigma})$  for the same  $\hat{s}$ , so we characterize the asymmetry of the reconstruction with respect to the disparity  $\hat{\sigma}$  as the asymmetry of the order parameter  $\hat{r}(\hat{\sigma})$  obtained in the simulation performed with  $\Delta\hat{\omega}(\hat{\sigma})$  and  $\Delta\hat{\omega}(-\hat{\sigma})$ :

$$\hat{A}(\hat{s}) = |\langle \hat{r}(\hat{\sigma}, \hat{s}) \rangle_T - \langle \hat{r}(-\hat{\sigma}, \hat{s}) \rangle_T|, \quad (11)$$

where  $\langle \hat{r}(\hat{\sigma}, \hat{s}) \rangle_T$  denotes the averaging over the time interval  $T$ . When the reconstruction is self-consistent and the time interval  $T$  is long enough the reconstructed asymmetry  $\hat{A}$  does not depend on the initial phases  $\theta_i(0)$  and, for a fixed disparity, decays with the coupling strength  $\hat{s}$  (Fig. 4). The exponential decay of  $\hat{A}(\hat{s})$  corresponds to the synchronized model with constant natural frequencies (Fig. 4, right), the power-law decay  $\hat{A} \sim 1/\hat{s}$  appears under desynchronization (Fig. 4, right), and the faster power-law decay  $\hat{A} \sim 1/\hat{s}^2$  corresponds to coherent oscillators with slowly variable natural frequencies.

We note, that the reconstructed asymmetry of the partial synchronization displayed in Fig. 4 (left) is higher than that of the desynchronization and synchronization. Let us now simulate the phase difference  $\alpha_i(t)$  in the chain model with the same natural frequencies  $\omega_i$  and coupling disparity  $\sigma$  and

growing coupling strength  $s$ . The asymmetry of the order parameter  $\hat{A}(s)$  reconstructed for a fixed coupling strength  $\hat{s}$  and the disparity  $\hat{\sigma} = \sigma$  is maximal when  $s$  reaches the boundary of synchronization  $s = s_{\text{max}}$  (Fig. 5). Generally, the decay of the reconstructed asymmetry  $\hat{A}(s)$  in the zone of synchronization has a power-law form (Fig. 5, right). Thus, comparing the reconstructed asymmetry for two chains we can conclude which of them is closer to the boundary of synchronization, assuming that both chains are on the same side of the synchronization threshold, and asymmetry is reconstructed with the same coupling parameters.

## 2. Application to the general model

The self-consistent reconstruction may be applied to each pair  $(i, j)$  of oscillators assuming that they are the edges of the chain. We take  $\alpha = (\theta_i - \theta_j)/2$  and use Eqs. (9) and (10) to reconstruct natural frequencies. In the chain model, we had a chance to reconstruct the true difference between natural frequencies  $\Delta\omega$  if oscillators are synchronized and the parameters are known  $\hat{s} = s$ ,  $\hat{\sigma} = \sigma$ ,  $\hat{\omega}_2 = \omega_2$ .

Reconstructing the difference between natural frequencies  $\Delta\omega = \omega_1 - \omega_3$  from the phase difference  $2\alpha = \theta_1 - \theta_3$  produced by a general model by applying the chain we get a systematic shift:

$$\Delta\hat{\omega} = \Delta\omega - 2\kappa_{13} \sin(\theta_1 - \theta_3). \quad (12)$$

However, when all oscillators are synchronized the shift  $2\kappa_{13} \sin(\theta_1 - \theta_3)$  is constant and does not affect the asymptotics of the reconstructed asymmetry  $\hat{A}$  for  $\hat{s} \rightarrow \infty$ .

It is more interesting how the reconstruction looks in the case of the partial synchronization. Let us consider the self-consistent reconstruction in the case of partially synchronized series simulated by the general model with constant natural frequencies. Figure 6 (top row) displays the evolution of the normalized difference between natural frequencies  $\Delta\hat{\omega}/\hat{s}$  reconstructed for intermediate  $\hat{s} = 2$  and large  $\hat{s} = 128$  coupling strength. When the coupling strength grows  $\Delta\hat{\omega}/\hat{s}$  for fixed  $\hat{\sigma}$  monotonously converges to the limit curve

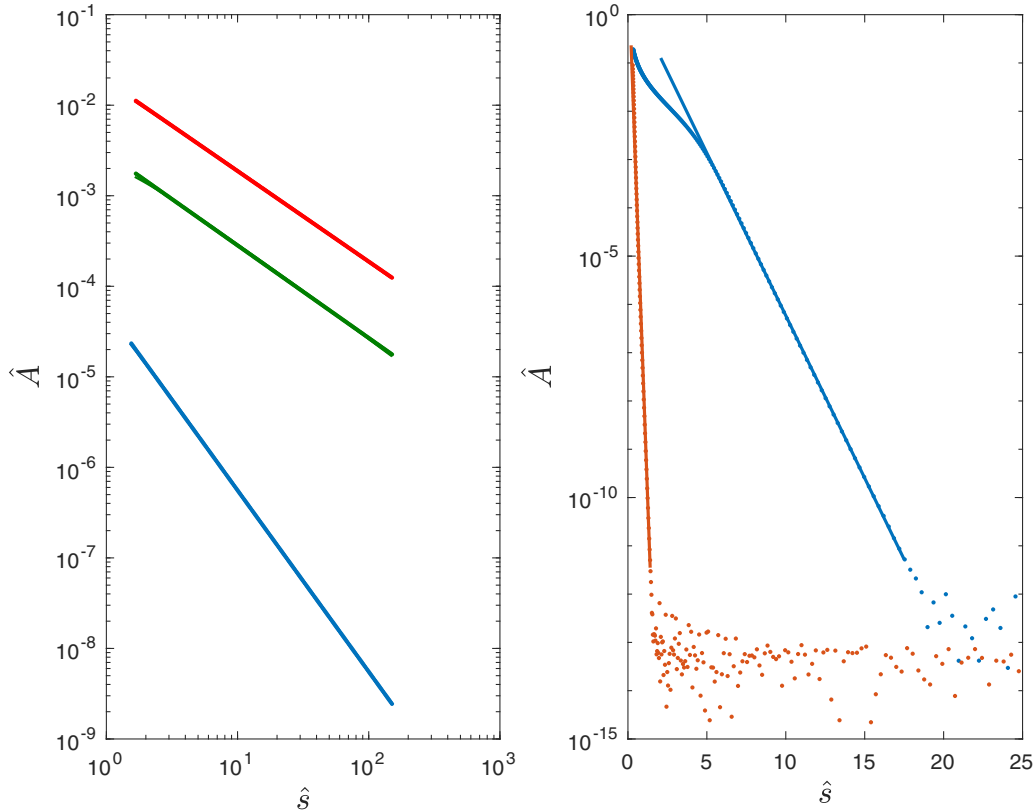


FIG. 4. Reconstructed asymmetry of the order parameter vs coupling strength  $\hat{s}$  of the reconstruction for the chain model with constant (right) and variable (left) natural frequencies. The power-law decay (left) is a general-case invariant, the exponential decay appears only for the synchronized oscillators with constant natural frequencies (right). Reconstruction is performed for  $\hat{\omega}_2=0$ ,  $\hat{\sigma} = 0.8$ . Right: The slope of the exponent depends on the coupling disparity  $\sigma = 0.8$  (blue),  $\sigma = 0.5$  (red) for fixed natural frequencies  $\omega_1 = 1.07$ ,  $\omega_2 = 0.29$ ,  $\omega_3 = 0.39$  and coupling strength  $s = 1$ . Left: Partial synchronization (red) and desynchronization (green) correspond to the scaling exponent  $g = 1$ . Synchronization (blue) correspond to the scaling exponent  $g = 2$ . Natural frequencies are  $\omega_1 = 1.07 + 0.2(1 + \sin 0.1t)$ ,  $\omega_2 = 0.29$ ,  $\omega_3 = 0.39$ , coupling corresponds to the zone of synchronization  $\sigma = 0.8$ ,  $s = 2$  (blue), partial synchronization  $\sigma = 0.8$ ,  $s = 0.5$  (red), and desynchronization  $\sigma = 0.8$ ,  $s = 0.2$  (green).

$\lim_{\hat{s} \rightarrow \infty} \Delta \hat{\omega}(t) / \hat{s} = D(t)$ , which reaches its maximum and minimum around the desynchronization event (Fig. 6, top middle and top right panels, solid blue line). Numerical calculation shows that the maximum  $D(t)$  is  $1 - |\hat{\sigma}|$  and the minimum is  $|\hat{\sigma}| - 1$ . These values are never reached for strong

$\hat{s}$  when there is no desynchronization and two oscillators are coherent, but may be eventually achieved for weak  $\hat{s}$  (Fig. 6, top left).

The middle row of Fig. 6 shows that the reconstruction is self consistent, original and simulated phase differences

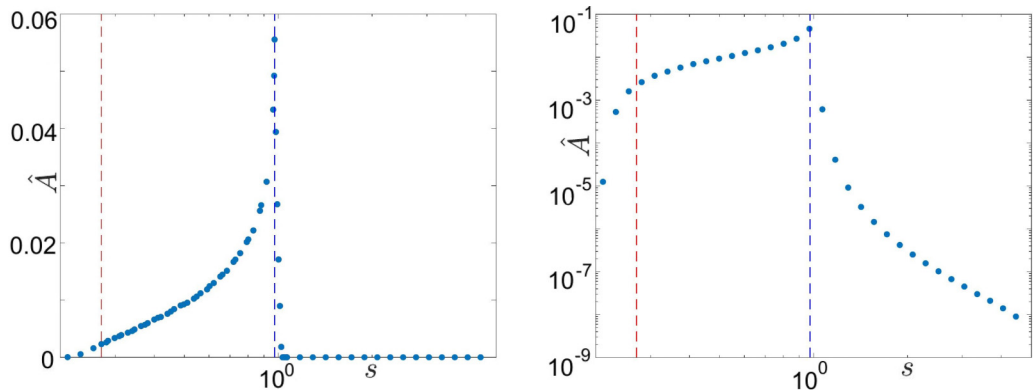


FIG. 5. Reconstructed asymmetry  $\hat{A}$  as a function of the original coupling strength  $s$  for constant (left) and evolving (right) natural frequencies. Vertical dashed lines indicate boundaries between partial synchronization and desynchronization (red) or synchronization (blue). Parameters of the reconstruction are  $\hat{s} = 2$ ,  $\hat{\sigma} = \sigma = 0.8$ . Natural frequencies are the same as on Fig. 4. Maximum of the reconstructed asymmetry is attained at the boundary of synchronization (vertical blue line).

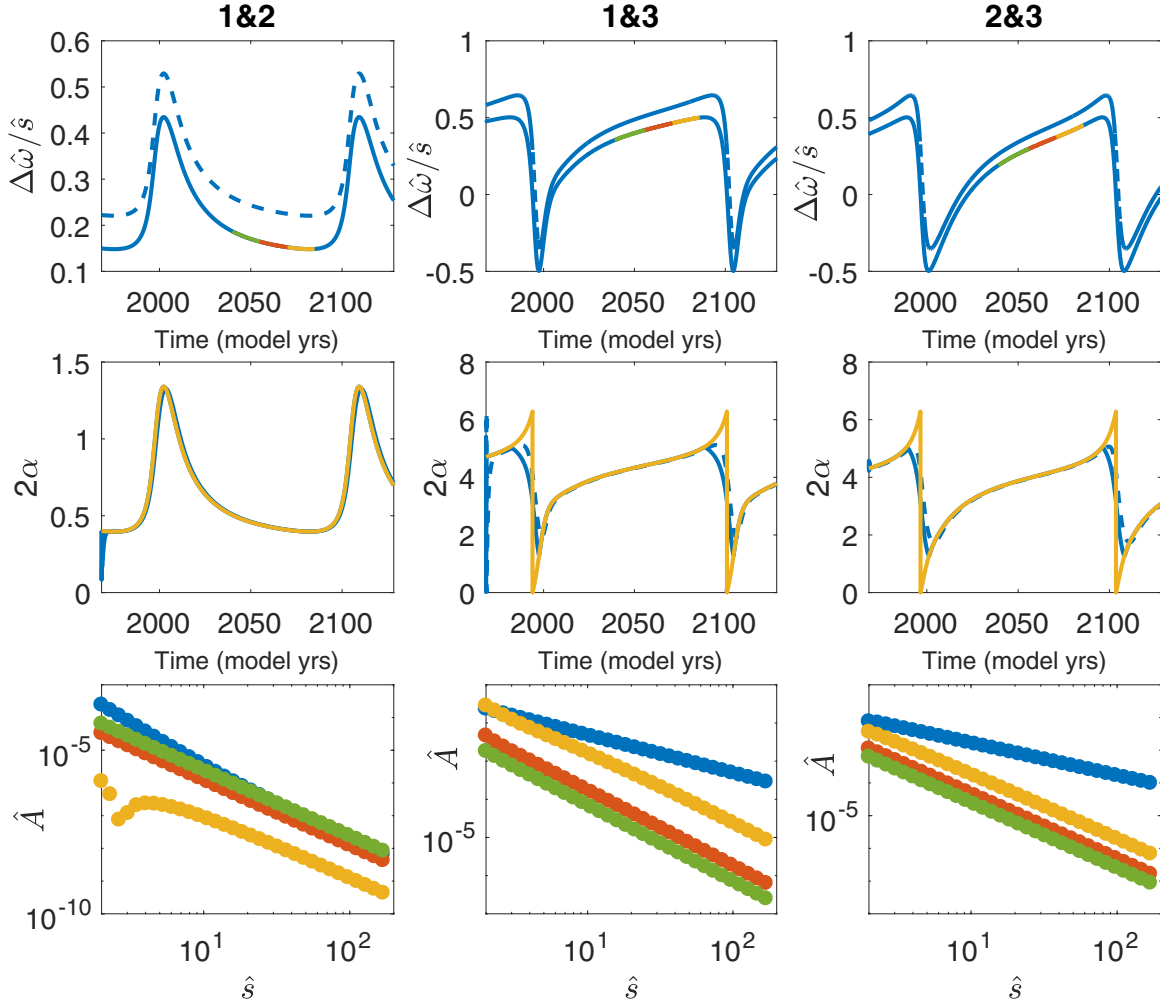


FIG. 6. Self consistent reconstruction with  $\hat{\sigma} = 0.5$  in the general model with constant natural frequencies ( $\omega_1 = 0.84$ ,  $\omega_2 = 0.45$ ,  $\omega_3 = 0.47$ ) and coupling ( $\kappa_{12} = \kappa_{21} = 0.25$ ,  $\kappa_{13} = \kappa_{31} = -0.15$ ,  $\kappa_{23} = \kappa_{32} = -0.05$ ). The model presents a partial synchronization: oscillators 1 and 2 are synchronized, the third oscillator drifts causing desynchronization events. Reconstruction is performed for three pairs of oscillators: (1,2), (1,3) and (2,3) (from left to right). Top row:  $\Delta\hat{\omega}/\hat{s}$  reconstructed for weak  $\hat{s} = 2$  and strong  $\hat{s} = 128$  coupling. Desynchronization events for  $\hat{s} = 128$  correspond to extremes of  $\Delta\hat{\omega}/\hat{s}$  equal to  $\pm(1 - |\hat{\sigma}|) = \pm 0.5$ . Middle row: self-consistency of the reconstruction, the original phase difference  $2\alpha = \theta_i - \theta_j$  (yellow) taken modulus  $2\pi$  is close to the phase difference reconstructed for  $\hat{s} = 2$  (dashed blue) and  $\hat{s} = 128$  (solid blue). The phase differences deviate near the desynchronization event. Bottom row: the reconstructed asymmetry  $\hat{A}$  vs coupling strength  $\hat{s}$  for the whole time interval (blue) and for three consecutive 15-year time intervals shown by the same colors on the top panels. The asymmetry curve is higher when the time interval is closer to the desynchronization event.

are similar outside the desynchronization episodes. The quick phase slip of the decoherence cannot be obtained by the reconstruction based on the hypothesis of synchronization.

The bottom row of Fig. 6 presents the reconstructed asymmetry  $\hat{A}(\hat{s})$  averaged over the time interval  $T$  derived for the same phase difference  $\alpha$  and increasing coupling strength  $\hat{s}$ . Asymmetry decays as  $1/\hat{s}^2$  when  $T$  does not include the desynchronization episode (Fig. 6, bottom left); otherwise, it decays as  $1/\hat{s}$  (Fig. 6, bottom middle and right, blue line). Let us note that convergence to  $1/\hat{s}^2$  or  $1/\hat{s}$  requires a large coupling strength  $\hat{s}$ . In addition to the full time interval  $T$  we consider three shorter consecutive intervals  $T_i$ ,  $i = 1, 2, 3$  approaching the desynchronization event (Fig. 6, top row, rectangles in green, red and yellow). We note that the asymmetry curve moves higher when we come closer to the desynchronization event (see points of the same color at the right panel of the middle and bottom rows of Fig. 6). Thus, we

see that the increase of asymmetry reconstructed for the same strong  $\hat{s}$  in the general model reflects proximity to the time of desynchronization by the same way as the increase of asymmetry in the chain model reflects closeness of the coupling strength  $s$  to the synchronization threshold  $s_{\max}$  (see Fig. 5).

### 3. Application to solar data

We consider the phase difference  $\Delta\Phi = \Phi_T - \Phi_P$  between the toroidal and the poloidal components of the solar magnetic field and use  $\alpha = \Delta\Phi/2$  to reconstruct natural frequencies from the self-consistent inverse problem. We assume that the natural frequency of the unobserved middle oscillator is zero  $\omega_2 = 0$ , and fix the unknown disparity  $\hat{\sigma} = 0.5$  as a parameter of the reconstruction performed for increasing coupling strength  $\hat{s}$ . The normalized difference  $\Delta\hat{\omega}/\hat{s}$  reaches its maximum  $1 - |\hat{\sigma}|$  and minimum  $|\hat{\sigma}| - 1$

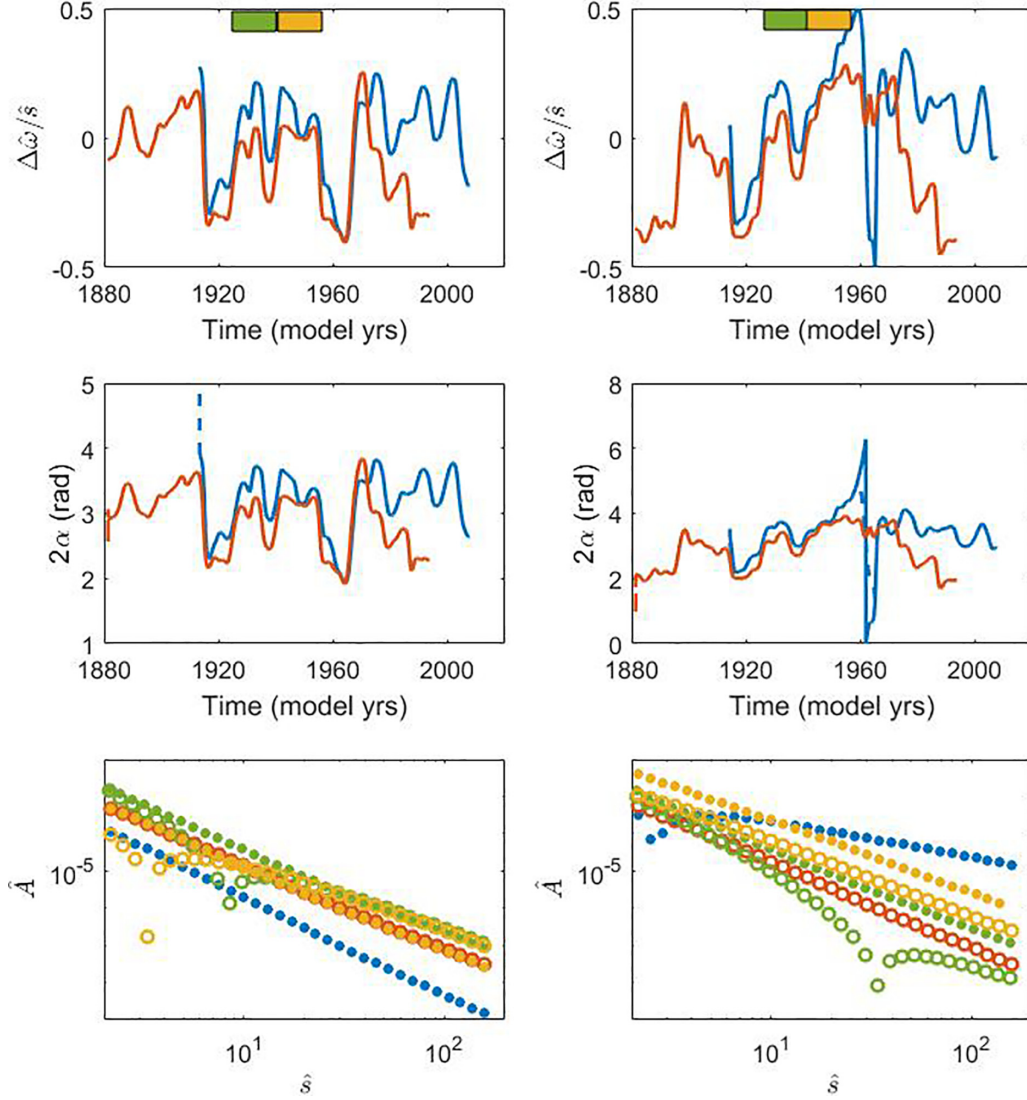


FIG. 7. The self-consistent reconstruction of solar data. Reconstruction is performed independently in the northern (left) and southern (right) hemispheres. Top row: normalized difference between natural frequencies  $\Delta\hat{\omega}/\hat{s}$  reconstructed with  $\hat{s} = 128$  and  $\hat{\sigma} = 0.5$  from the phase difference  $\alpha_m(t)$  (blue) and  $\alpha_p(t)$  (red). The desynchronization event in the southern hemisphere (right panel, blue line) corresponds to the  $\Delta\hat{\omega}/\hat{s} = 1 - \hat{\sigma} = 0.5$ . Middle row: comparison of the simulated phase difference (dashed) with the original one (solid) taken in  $[0, 2\pi]$  for  $\alpha_m(t)$  (blue) and  $\alpha_p(t)$  (red). Apart from the start point and desynchronization event in the southern hemisphere, the simulated and the original phase differences coincide proving the self-consistency. Bottom row: Asymmetry  $\hat{A}$  derived from  $\alpha_m(t)$  (blue full circle) and  $\alpha_p(t)$  (red open circles) on the whole time interval of observations (blue), and 15-year time intervals  $T_1 = [1925-1940]$  (green) and  $T_2 = [1940-1955]$  (yellow). In the southern hemisphere (right) asymmetry curve is higher when the time interval is closer to the desynchronization event.

during the desynchronization event in 1960 observed in the southern hemisphere for MWO/WSO data (Fig. 7, top right panel, blue line).

The two series of polar faculae (MWO/WSO and Pulkovo data) determine two series of phase differences  $\alpha_m(t) = (\Phi_T - \Phi_{Pm})/2$  and  $\alpha_p(t) = (\Phi_T - \Phi_{Pp})/2$ , respectively, in each of the two solar hemispheres (the northern and the southern one); see Fig. 7, middle row. The reconstruction is indeed self-consistent apart from the desynchronization event of 1960, where the model (blue dashed line) differs from the original (blue solid line) phase difference due to the violation of the synchronization assumption.

Asymmetry  $A$  is derived from the phase difference  $\alpha$  and decays as  $1/\hat{s}^g$  when the coupling strength  $\hat{s}$  is large enough.

The scaling is close to 1 when the desynchronization event is present (MWO/WSO data in the southern hemisphere) and close to 2 otherwise (see Table I). Apart from the full-time span we compare two 15-year intervals of time [1925–1940]

TABLE I.  $g$ -values of asymmetry derived from solar data.

Time interval	North		South	
	MWO/WSO	Pulkovo	MWO/WSO	Pulkovo
Full time	2.32	2.06	0.99	2.11
1925–1940	2.06	1.94	2.03	1.67
1940–1955	2.08	1.95	1.99	2.01



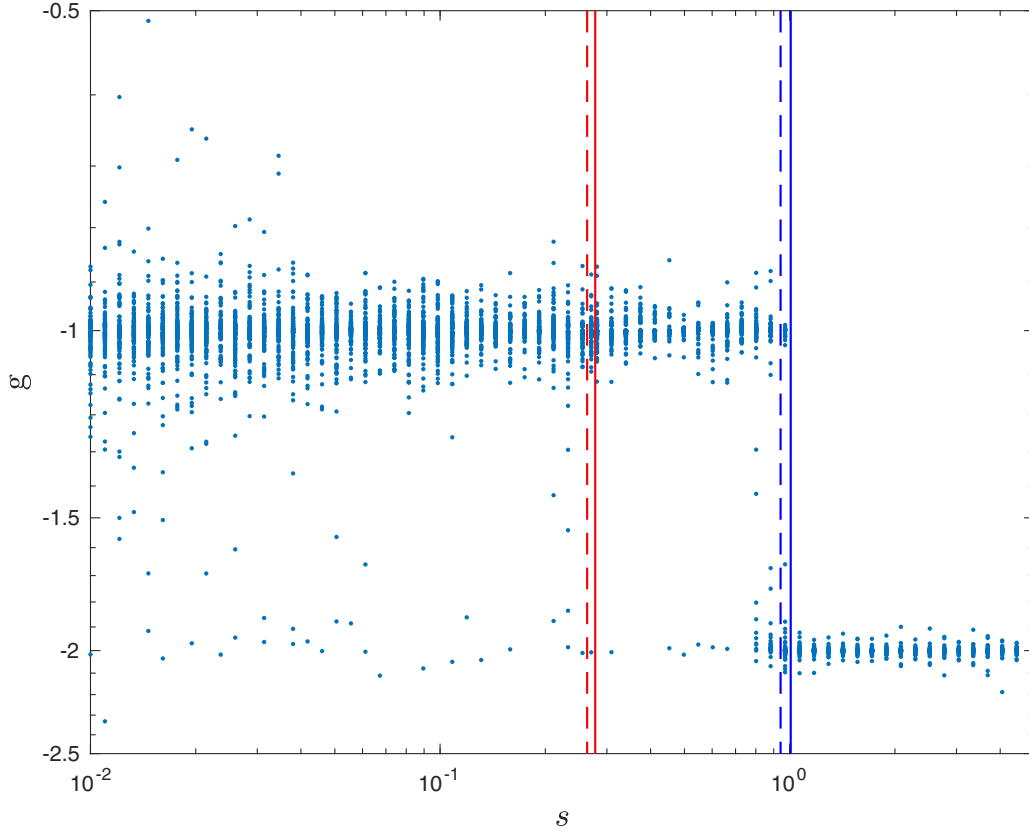


FIG. 8. Influence of the finite interval of observations to the variability of the scaling exponent  $g$ . Asymmetry  $A$  for each  $s$  is reconstructed from the 110 consecutive time series of phase differences  $\alpha(t)$  where  $t \in [T_n, T_n + T]$ ,  $n = 1, \dots, 110$  simulated by the chain model with coupling strength  $s$  and disparity  $\sigma = 0.8$ . Reconstruction is performed with  $\hat{\sigma} = 0.2$ . Natural frequencies are the same as in Fig. 4, left. Vertical lines show theoretical boundaries of the coupling strength between desynchronization and partial synchronization (red) and between partial synchronization and synchronization (blue). The difference between minimal and maximal boundaries (dashed and solid line, respectively) appears due to variable natural frequencies. Near the boundary of the synchronization both exponents  $g = 1$  and  $g = 2$  are present.

and [1940–1955] (green and yellow rectangles in the top row of Fig. 7) to see how the asymmetry changes in the proximity of the desynchronization event. Although the scaling  $g$  remains close to 2, the asymmetry grows when the time interval is closer to the desynchronization event in 1960 (compare green and yellow full circles in the bottom right panel of Fig. 7). The increase of asymmetry before the desynchronization event agrees with the model (see Fig. 6). The deviation of scaling  $g = 1.67$  observed for Pulkovo data for the time span [1925–1940] (see Table I) is related with insufficiently large  $s$ , convergence is not yet achieved (see Fig. 7, bottom right, green open circles).

### III. RESULTS

#### A. Decoherence corresponds to $\hat{A} \sim 1/\hat{s}$

We find that the decay of the reconstructed asymmetry  $\hat{A}(\hat{s})$  with the coupling strength  $\hat{s}$  is determined by the coherence between two considered oscillators observed within the time interval  $T$ . If two oscillators at any time interval within  $T$  became desynchronized then the reconstructed asymmetry  $\hat{A}(\hat{s})$  always decays as  $1/\hat{s}^g$  with  $g = 1$  (Fig. 4, left presents examples of numerical simulation for the chain model). The exponent  $g = 1$  is an invariant reached numerically if  $T$  is

long enough for all disparities  $\hat{\sigma}$  in either chain or general model. Numerical simulations with finite values of  $T$  result in the exponent  $g$  distributed around  $g = 1$  (Fig. 8).

#### B. Coherence corresponds to $\hat{A} \sim 1/\hat{s}^2$

Although the reconstructed asymmetry in the chain model with synchronized oscillators and constant natural frequencies demonstrate an exponential decays with coupling strength  $s$  (Fig. 4, right), this kind of behavior appears to be rather exceptional. In the chain model with variable natural frequencies, the synchronization corresponds to  $\hat{A} \sim 1/\hat{s}^2$  (the blue line in Fig. 4, left). In the general model with constant natural frequencies a synchronized pair provides  $\hat{A} \sim 1/\hat{s}^2$  if the third oscillator is drifting (Fig. 6, top row). We even observe  $\hat{A} \sim 1/\hat{s}^2$  in the case of partial synchronization when observations are contained within a finite time interval of quasicoherece (compare, e.g., yellow and blue line at Fig. 6, bottom middle and right panels, Fig. 7, bottom right). This effect explains why both scaling exponents  $g = 2$  and  $g = 1$  are simultaneously present near the boundary of synchronization if the reconstruction is performed on a finite time interval (Fig. 8, just on the left-hand side of the vertical blue line).

### C. Asymmetry increases before the desynchronization event

The reconstructed asymmetry is maximal near the boundary between synchronization and partial synchronization (Fig. 5). As a result, the reconstructed asymmetry increases when the system on a finite time interval comes close to this boundary (compare green, red and yellow lines at Fig. 6, bottom middle and right panels, green and yellow lines at Fig. 7, bottom right panel). Although  $\hat{A} \sim 1/\hat{s}^2$  both for synchronized and desynchronized pairs of oscillators, the increase of asymmetry reflects the approaching desynchronization event (compare left and right panels of Fig. 6 or Fig. 7).

## IV. DISCUSSION

Partial synchronization, chimera, or solitary states appear between the synchronized and desynchronized regimes in various oscillatory systems [34]. In practice, one deals with observations, where occasional events of desynchronization (or synchronization) appears in the normally coherent (decoherent) evolution. Apart from understanding the origin of such events there is a need of their identification and prediction. While there are mathematical tools to separate, e.g., true chimera from weak ones, most observations, e.g., of solar indices, do not provide long enough series to see a difference. The term “partial synchronization” used in the present study corresponds to solitary states [35,36,47] because the true chimera has not been observed within one century record of solar data.

In our previous work [15], we related the desynchronization event in solar proxies, occurred in the 1960s, with variations of the meridional flow speed. The present study shows that the desynchronization event is reflected in the reconstructed natural frequencies even when the original ones do not change at all. The self-consistent reconstruction compensates the depart from synchrony through the difference between reconstructed natural frequencies  $\Delta\hat{\omega}(t)/\hat{s}$ . The limit  $D(t) = \lim_{\hat{s} \rightarrow \infty} \Delta\hat{\omega}(t)/\hat{s}$  reaches the extremum near the desynchronization event both in model (Fig. 6) and solar data (Fig. 7), which may be used as an indicator of desynchronization. Unfortunately,  $D(t)$  does not predict the following desynchronization event. In contrast, the asymmetry  $\hat{A}(\hat{s})$  as the function of coupling strength reconstructed on a time interval  $T$  exhibits the decay  $s^{-2}$  or  $s^{-1}$  if  $T$  does not include or, respectively, includes the desynchronization episode. Therefore,  $\hat{A}(\hat{s})$  undergoes a transition to the  $s^{-1}$  decay prior to the desynchronization episode, which is observed with a general uplift of the  $\hat{A}(\hat{s})$ -curve. Thus, the derived asymmetry  $\hat{A}$  may be of use for the prediction of the desynchronization between the solar indices.

The simple Kuramoto model studied in this paper gives just an example of how the coupling asymmetry may be used for the indication and prediction of the occasional decoherence between oscillators. The true origin of the decoherence may be unknown but the same approach is applicable if the

asymmetry is given. For example, the asymmetry of the coupling natural frequencies appears in the Kuramoto-Sakaguchi model because of delay [47,48] or it may be the result of a directed network [36]. Although we consider models with three oscillators, we believe that similar technique may be applied for a larger system by taking individual pairs of oscillators as two edges of an imaginary chain.

## ACKNOWLEDGMENTS

We are grateful to two anonymous reviewers for very constructive comments.

## APPENDIX A: GENERALIZED ORDER PARAMETER IN THE KURAMOTO CHAIN WITH THREE OSCILLATORS

The classical Kuramoto model of  $N$  oscillators coupled with strength  $K > 0$  may be reduced to the mean-field equation

$$\dot{\theta}_i = \omega_i + KR \sum_{j=1}^N \sin(\Psi - \theta_j), \quad (\text{A1})$$

where  $R$  and  $\Psi$  denote the order parameter and the mean phase, respectively:

$$\text{Re}^{i\Psi} = \frac{1}{N} \sum_{j=1}^N \theta_j. \quad (\text{A2})$$

The order parameter  $0 < R < 1$  appears to be a good measure of synchronization [2].

Despite its simplicity, the chain presented in Sec. II A 1 has two complications: first, it is a network, and one of the coupling coefficients is zero. Second, the two nonzero coupling coefficients are not equal  $q_1 \neq q_2$  and do not have to be positive. To get the order parameter for nonequal coupling coefficients we combine the idea of weighted sum of local order parameters proposed by Ichinomiya [49] with the order parameter  $r_{\text{uni}}$  introduced by Schröder *et al.* [39]. Although, the difference in the definition of the order parameter may be essential for the mean field analysis of large systems with  $N \rightarrow \infty$  [50], for our purpose and small system ( $N = 3$ ) any definition is good as long as it reflects the phase transition between partial synchronization and synchronization (see comparison in Schröder *et al.* [39]). We modify the order parameter  $r_{\text{uni}}$  introduced by Schröder *et al.* [39] for a network:

$$r_{\text{uni}} = -\frac{\sum_{j=1}^N \lambda_j}{K \sum_{j=1}^N k_i} = -\frac{\text{tr}(J)}{K \sum_{j=1}^N k_i}, \quad (\text{A3})$$

where  $k_i$  denote the degree of the node  $i$ , and  $\lambda_j$  are eigenvalues of the Jacobian  $J$  of the system (1) under condition of constant natural frequencies  $\omega_i = \text{const}$ . For the chain model given by Eq. (1) the Jacobian  $J$  is

$$J = \begin{pmatrix} -q_1 \cos(\theta_1 - \theta_2) & q_1 \cos(\theta_1 - \theta_2) & 0 \\ q_1 \cos(\theta_1 - \theta_2) & -q_1 \cos(\theta_1 - \theta_2) - q_2 \cos(\theta_2 - \theta_3) & q_2 \cos(\theta_2 - \theta_3) \\ 0 & q_2 \cos(\theta_2 - \theta_3) & -q_2 \cos(\theta_2 - \theta_3) \end{pmatrix}. \quad (\text{A4})$$

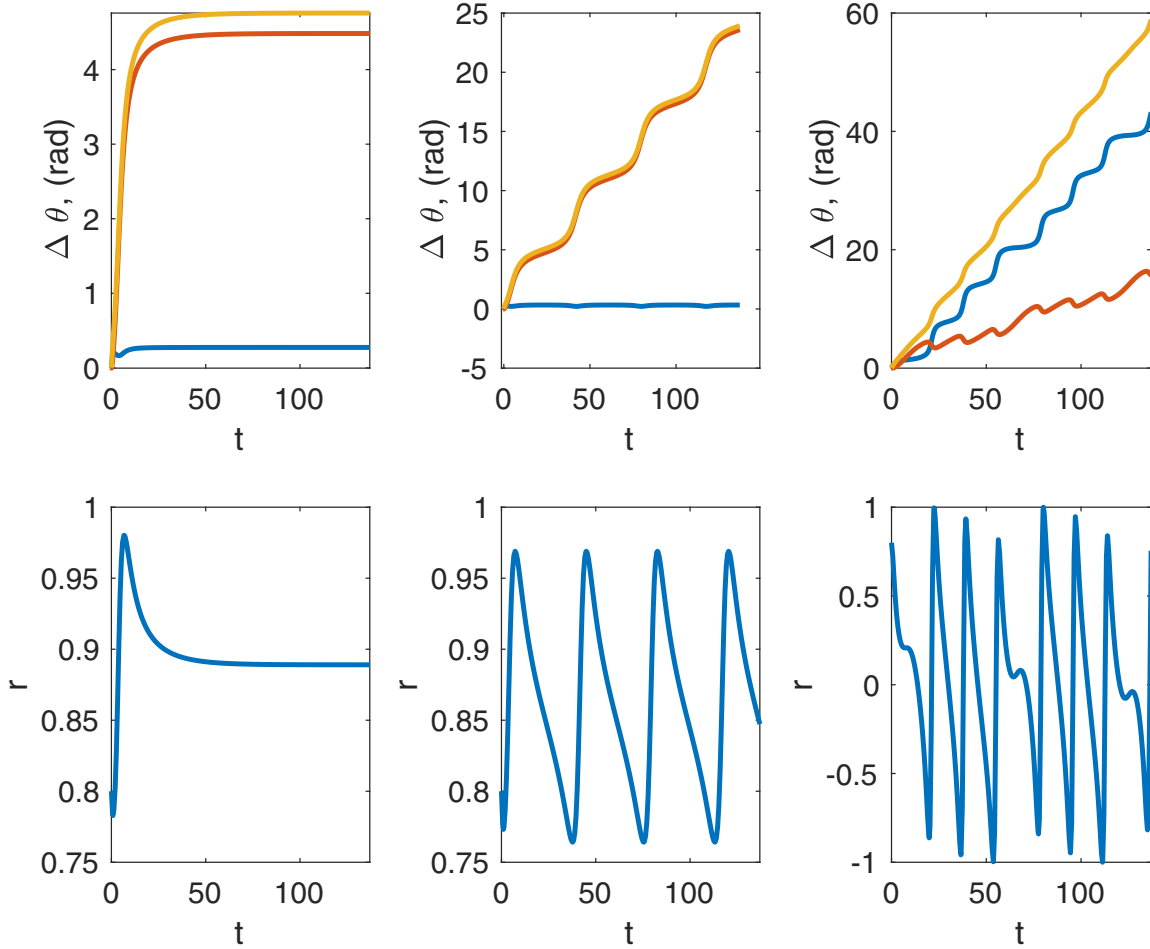


FIG. 9. Evolution of the phase differences (top row) and the order parameter (bottom row) in a chain of three Kuramoto oscillators. From left to right: phase-locking when coupling coefficients have different signs, partial synchronization, desynchronization. Colors of the top row indicate phase difference between oscillators  $\theta_1 - \theta_2$  (blue),  $\theta_2 - \theta_3$  (red),  $\theta_1 - \theta_3$  (yellow). Simulation is performed for  $\omega_1 = 1.07$ ,  $\omega_2 = 0.29$ ,  $\omega_3 = 0.39$ ,  $\sigma = 0.8$ , and  $s = |\Delta k|$  taking value  $s = 1$  (left),  $s = 0.8$  (middle), and  $s = 0.2$  (right).

We substitute  $tr(J)$  in the nominator of Eq. (A3). In the chain model with three oscillators  $k_1 = k_3 = 1$  and  $k_2 = 2$ . Generalizing the denominator  $K \sum_{j=1}^3 k_j$  in the order parameter (A3) to nonidentical coupling coefficient and substituting to Eq. (A3) we get

$$r = \frac{q_1 \cos(\theta_1 - \theta_2) + q_2 \cos(\theta_2 - \theta_3)}{|q_1| + |q_2|}. \quad (\text{A5})$$

Clearly, Eq. (A5) is reduced to Eq. (A3) when coupling coefficients are identical  $q_1 = q_2 = K$ . In opposite to the classical order parameter of  $r_{\text{uni}}$  the order parameter given by  $r_{\text{uni}}$ (A5) does depend on the coupling values. However, a stable phase-locking corresponds to the negative eigenvalues  $\lambda_j < 0$  and ensures  $0 \leq r \leq 1$  for all coupling coefficient. The generalized order parameter (4) is now defined for positive and negative values of coupling, which yields the coincidence of  $r$  with the real part of the classical order parameter in the case of identical couplings  $\kappa_{ij} = K$  [2].

Synchronization is defined in the Kuramoto models as the convergence of all frequencies of the oscillators  $\dot{\theta}_i$  to the same frequency  $\Omega$  [2] or as an asymptotic phase locking  $\theta_i - \theta_j \rightarrow \text{const}$  [3]. When all coupling coefficients are equal  $\kappa_{ij} = K$ , synchronization always appears when the coupling is strong

$K > K_{\text{cr}}$  and the mean frequency  $\Omega$  is equal to the average natural frequency of all oscillators. The order parameter in the case of synchronization converges to a limit  $R > 0$  but its behavior outside the synchronization area is still unclear [51]. Since we consider symmetrical coupling  $\kappa_{ij} = \kappa_{ji}$ , the frequency of synchronization is also equal to the mean natural frequency  $\Omega = \frac{1}{3} \sum \omega_i$  [it follows from the sum of Eqs. (1)]. Numerical exploration of the model with constant natural frequencies and coupling coefficients  $q_1 \neq q_2$  reveals three kinds of model dynamics (see illustrative examples in Fig. 9): synchronization, partial synchronization and desynchronization.

(1) Synchronization of all three oscillators:  $\dot{\theta}_i(t) \rightarrow \Omega$ , oscillators are coherent and asymptotically phase locked  $[\theta_i(t) - \theta_j(t)]/2 \rightarrow \alpha_{ij} = \text{const}$ . Synchronization corresponds to the constant positive order parameters (Fig. 9, left column). Let us note that taking modulus  $2\pi$  in the interval  $[-\pi, \pi]$  the phase difference  $2\alpha$  satisfies  $|2\alpha| < \pi/2$  or  $|2\alpha| > \pi/2$ , depending on the signs of coupling coefficients and the relationship between  $k = (q_1 + q_2)/2$  and  $\Delta k = (q_1 - q_2)/2$  [red and blue triangles, respectively, on Fig. 10)]. The boundaries of the synchronization zone may be obtained analytically. Let us rewrite Eq. (1) for the phase

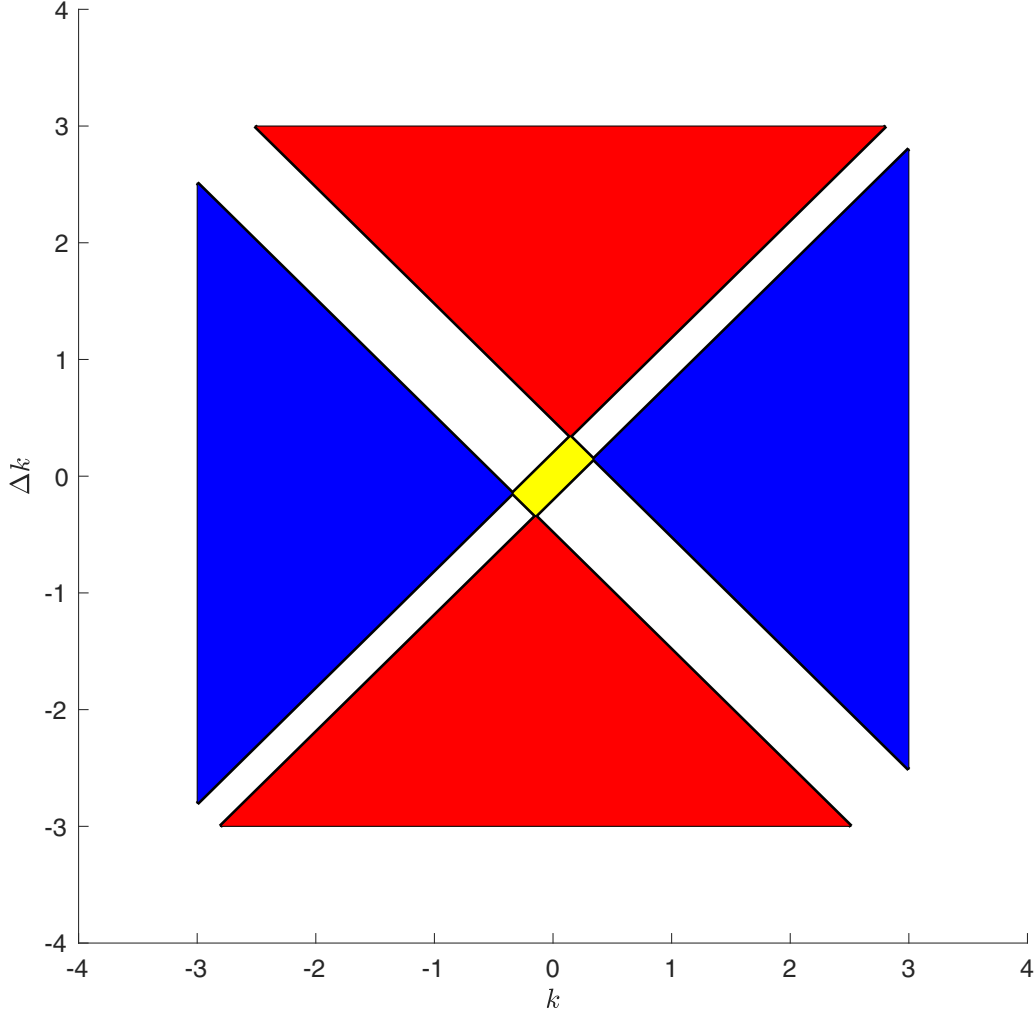


FIG. 10. Phase diagram of synchronization for a chain of three Kuramoto oscillators. Coupling domains, where three oscillators are phase-locked (red and blue zones), none of oscillators are phase locked (yellow rectangle), two of three oscillators are phase-locked (white zones outside the central rectangle). Synchronization corresponds to the stable phase difference  $\theta_1 - \theta_3 = 2\alpha$  taken from  $-\pi$  to  $\pi$  where  $2|\alpha| < \pi/2$  (red zones) and  $2|\alpha| > \pi/2$  (blue zones). Natural frequencies are  $\omega_1 = 1.07$ ,  $\omega_2 = 0.29$ ,  $\omega_3 = 0.39$ .

differences  $\alpha = (\theta_1 - \theta_3)/2$  and  $\beta = (\theta_1 + \theta_3)/2 - \theta_2$ :

$$\begin{aligned} \dot{\alpha} &= \Delta\omega - k \sin \alpha \cos \beta - \Delta k \sin \beta \cos \alpha, \\ \dot{\beta} &= \frac{3}{2}(\Omega - \omega_2) - 3k \sin \beta \cos \alpha - 3\Delta k \sin \alpha \cos \beta, \end{aligned} \quad (\text{A6})$$

where  $\Delta\omega = (\omega_1 - \omega_3)/2$  denotes the difference between natural frequencies of the two edge oscillators. Synchroniza-

tion requires the phase locking:

$$\lim_{t \rightarrow \infty} \dot{\alpha}(t) = 0, \quad \lim_{t \rightarrow \infty} \dot{\beta}(t) = 0. \quad (\text{A7})$$

The phase-locked stationary solution  $\alpha(t) = \tilde{\alpha}$ ,  $\beta(t) = \tilde{\beta}$  of Eq. (A6) satisfies equations

$$\sin(\tilde{\alpha} - \tilde{\beta}) = \frac{\Delta\omega - \frac{\Omega - \omega_2}{2}}{(k - \Delta k)}, \quad \sin(\tilde{\alpha} + \tilde{\beta}) = \frac{\Delta\omega + \frac{\Omega - \omega_2}{2}}{(k + \Delta k)}. \quad (\text{A8})$$

The stationary solution  $\alpha(t) = \tilde{\alpha}$ ,  $\beta(t) = \tilde{\beta}$  is stable when the Jacobian  $J^*$  of Eq. (A6),

$$J^* = \begin{pmatrix} -k \cos \tilde{\alpha} \cos \tilde{\beta} + \Delta k \sin \tilde{\alpha} \sin \tilde{\beta} & k \sin \tilde{\alpha} \sin \tilde{\beta} - \Delta k \cos \tilde{\alpha} \cos \tilde{\beta} \\ 3k \sin \tilde{\alpha} \sin \tilde{\beta} - 3\Delta k \cos \tilde{\alpha} \cos \tilde{\beta} & -3k \cos \tilde{\alpha} \cos \tilde{\beta} + 3\Delta k \sin \tilde{\alpha} \sin \tilde{\beta} \end{pmatrix}, \quad (\text{A9})$$

has negative eigenvalues, which requires the coefficients of the characteristic equation

$$\lambda^2 + 4\lambda(k \cos \tilde{\alpha} \cos \tilde{\beta} - \Delta k \sin \tilde{\alpha} \sin \tilde{\beta}) + 3[(-k \cos \tilde{\alpha} \cos \tilde{\beta} + \Delta k \sin \tilde{\alpha} \sin \tilde{\beta})^2 - (k \sin \tilde{\alpha} \sin \tilde{\beta} - \Delta k \cos \tilde{\alpha} \cos \tilde{\beta})^2] = 0 \quad (\text{A10})$$

to be positive. The second coefficient is

$$k \cos \tilde{\alpha} \cos \tilde{\beta} - \Delta k \sin \tilde{\alpha} \sin \tilde{\beta} = (k + \Delta k) \cos(\tilde{\alpha} + \tilde{\beta}) + (k - \Delta k) \cos(\tilde{\alpha} - \tilde{\beta}) > 0. \quad (\text{A11})$$

The third coefficient is

$$(-k \cos \tilde{\alpha} \cos \tilde{\beta} + \Delta k \sin \tilde{\alpha} \sin \tilde{\beta})^2 - (k \sin \tilde{\alpha} \sin \tilde{\beta} - \Delta k \cos \tilde{\alpha} \cos \tilde{\beta})^2 = (k - \Delta k) \cos(\tilde{\alpha} - \tilde{\beta})(k + \Delta k) \cos(\tilde{\alpha} + \tilde{\beta}) > 0. \quad (\text{A12})$$

Combining conditions (A11) and (A12) we get

$$(k + \Delta k) \cos(\tilde{\alpha} + \tilde{\beta}) > 0 \quad \text{and} \quad (k - \Delta k) \cos(\tilde{\alpha} - \tilde{\beta}) > 0. \quad (\text{A13})$$

When  $|k| > |\Delta k|$  stable stationary solution  $\tilde{\alpha} = \lim_{t \rightarrow \infty} \alpha(t)$  and  $\tilde{\beta} = \lim_{t \rightarrow \infty} \beta(t)$  of Eq. (A6) has the phase difference  $2\tilde{\alpha}$  considered modulus  $2\pi$  close to 0 ( $|2\tilde{\alpha}| < \pi/2$ ). When  $|k| < |\Delta k|$  the phase difference is close to  $\pi$  ( $|\pi - 2\tilde{\alpha}| < \pi/2$ ) (see Theorem 2 in Appendix C Conditions (A13) and (A8) determine the following boundaries of coupling domains (four shaded zones in Fig. 10) where there exist a phase locking of three oscillators (Fig. 9, left):

$$\begin{aligned} |k + \Delta k| &= \left| \Delta\omega + \frac{\Omega - \omega_2}{2} \right|, \\ |k - \Delta k| &= \left| \Delta\omega - \frac{\Omega - \omega_2}{2} \right| \end{aligned} \quad (\text{A14})$$

(2) Partial synchronization: two oscillators are coherent and one drifts away. Partial synchronization corresponds to the quasiconstant phase difference between two synchronized oscillators and oscillating positive order parameter (Fig. 9, middle column). The partial synchronization appears when  $k$  and  $\Delta k$  are close. Its boundaries with the synchronization zone are given by Eq. (A14).

(3) Desynchronization is characterized by decoherent behavior of all three oscillators. It corresponds to chaotic

variations of the order parameter reaching even negative values (Fig. 9, right column). Desynchronization appears when the coupling strength is small (the yellow rectangle at Fig. 10).

Equations (A14) allow us to express the thresholds of synchronization  $s > s_{\max}$  and desynchronization  $s < s_{\min}$  for fixed disparity  $\sigma$  as

$$\begin{aligned} s_{\max} &= \max \left( \frac{|\Delta\omega + \frac{\Omega - \omega_2}{2}|}{1 + \sigma}, \frac{|\Delta\omega - \frac{\Omega - \omega_2}{2}|}{1 - \sigma} \right), \\ s_{\min} &= \min \left( \frac{|\Delta\omega + \frac{\Omega - \omega_2}{2}|}{1 + \sigma}, \frac{|\Delta\omega - \frac{\Omega - \omega_2}{2}|}{1 - \sigma} \right), \end{aligned} \quad (\text{A15})$$

## APPENDIX B: ASYMMETRY OF THE ORDER PARAMETER IN THE CHAIN OF THREE OSCILLATORS: DIRECT PROBLEM

Let us rewrite Eq. (A6) with respect to coupling strength  $s$  and coupling disparity  $\sigma$ :

$$\begin{aligned} \frac{\Delta\omega}{s} - \frac{\dot{\alpha}}{s} &= \begin{cases} \sin \alpha \cos \beta + \sigma \sin \beta \cos \alpha, & s = |k|, \\ \sigma \sin \alpha \cos \beta + \sin \beta \cos \alpha, & s = |\Delta k|, \end{cases} \\ \frac{(\Omega - \omega_2)}{2s} - \frac{\dot{\beta}}{3s} &= \begin{cases} \sin \beta \cos \alpha + \sigma \sin \alpha \cos \beta, & s = |k|, \\ \sigma \sin \beta \cos \alpha + \sin \alpha \cos \beta, & s = |\Delta k|, \end{cases} \end{aligned} \quad (\text{B1})$$

which for  $s = |k|$  is easily transformed to

$$\begin{aligned} \sin(\alpha + \beta)(1 + \sigma) &= \frac{\Delta\omega}{s} + \frac{\Omega - \omega_2}{2s} - \frac{3\dot{\alpha} + \dot{\beta}}{3s}, \\ \sin(\alpha - \beta)(1 - \sigma) &= \frac{\Delta\omega}{s} - \frac{\Omega - \omega_2}{2s} - \frac{3\dot{\alpha} - \dot{\beta}}{3s}, \end{aligned} \quad (\text{B2})$$

and for  $s = |\Delta k|$  we get the opposite sign in the last equation:

$$\begin{aligned} \sin(\alpha + \beta)(1 + \sigma) &= \frac{\Delta\omega}{s} + \frac{\Omega - \omega_2}{2s} - \frac{3\dot{\alpha} + \dot{\beta}}{3s}, \\ -\sin(\alpha - \beta)(1 - \sigma) &= \frac{\Delta\omega}{s} - \frac{\Omega - \omega_2}{2s} - \frac{3\dot{\alpha} - \dot{\beta}}{3s}. \end{aligned} \quad (\text{B3})$$



It follows from Eq. (B1) that when natural frequencies are constant and the system is synchronized ( $\dot{\alpha} \rightarrow 0$ ,  $\dot{\beta} \rightarrow 0$ ) then  $\sin(\alpha + \beta)$  and  $\sin(\alpha - \beta)$  decay as  $1/s$ . Consequently, in the first order,

$$\cos(\alpha + \beta) \sim 1 - 1/s^2, \quad \cos(\alpha - \beta) \sim 1 - 1/s^2, \quad (\text{B4})$$

both for positive and negative  $\sigma$ .

Asymmetry of the order parameter is expressed from Eq. (5) as

$$A = \begin{cases} \left| \frac{1+\sigma}{2} [\cos(\alpha^+ + \beta^+) - \cos(\alpha^- - \beta^-)] + \frac{1-\sigma}{2} [\cos(\alpha^+ - \beta^+) - \cos(\alpha^- + \beta^-)] \right|, & s = |k|, \\ \left| \frac{1+\sigma}{2} [\cos(\alpha^+ + \beta^+) - \cos(\alpha^- - \beta^-)] - \frac{1-\sigma}{2} [\cos(\alpha^+ - \beta^+) - \cos(\alpha^- + \beta^-)] \right|, & s = |\Delta k|, \end{cases} \quad (\text{B5})$$

where  $\alpha^+$ ,  $\beta^+$  and  $\alpha^-$ ,  $\beta^-$  denote phase differences relevant to  $\sigma$  and  $-\sigma$ , respectively. It follows from Eqs. (B2) and (B3) that for  $\Omega \neq \omega_2$  the cosines  $\cos(\alpha^+ + \beta^+)$  and  $\cos(\alpha^- - \beta^-)$  cannot be equal because absolute values of their sines are different. The same is true for cosines  $\cos(\alpha^+ - \beta^+)$  and  $\cos(\alpha^- + \beta^-)$ . Substituting in Eq. (B5) the asymptotic values of cosines from Eq. (B4) we get that asymmetry of the order parameter decays at least as  $1/s^2$ . On the contrary, when  $\Omega = \omega_2$  the sines became equal  $\sin(\alpha^+ + \beta^+) = \sin(\alpha^- - \beta^-)$ ,  $\sin(\alpha^+ - \beta^+) = \sin(\alpha^- + \beta^-)$  and asymmetry of the order parameter becomes zero.

### APPENDIX C: INVERSE PROBLEM IN A CHAIN OF THREE OSCILLATORS

Let us now consider the inverse problem for the chain of  $N = 3$  oscillators (see Sec. II A 1). We assume that all oscillators are synchronized to the mean frequency  $\Omega$ , the natural frequency  $\omega_2$  is given, and phases of the two edge oscillators  $\tilde{\theta}_1 = \lim_{t \rightarrow \infty} \theta_1(t)$  and  $\tilde{\theta}_3 = \lim_{t \rightarrow \infty} \theta_3(t)$  are observed. We aim to reconstruct natural frequencies  $\omega_1$  and  $\omega_3$  using coupling coefficients  $k = \hat{k}$  and  $\Delta k = \Delta \hat{k}$ . The reconstruction is performed in two steps: first, we reconstruct the unknown phase difference  $\beta$  using the assumption of the phase locking, and second, we reconstruct natural frequencies.

#### 1. Reconstruction of the unknown phase difference

It follows from Eq. (A6) that for the known phase difference  $\alpha(t) = \tilde{\alpha} \in [-\pi/2, \pi/2]$  the unknown phase difference  $\hat{\beta} = \lim_{t \rightarrow 0} \beta(t)$  must be a stable stationary solution of the differential equation:

$$\dot{\beta} = \frac{3}{2}(\Omega - \omega_2) - 3\hat{k} \cos \tilde{\alpha} \sin \beta - 3\Delta \hat{k} \sin \tilde{\alpha} \cos \beta. \quad (\text{C1})$$

After simple transformation we obtain

$$\cos(\hat{\beta} + \gamma) = \frac{\Omega - \omega_2}{2\sqrt{(\Delta \hat{k} \sin \tilde{\alpha})^2 + (\hat{k} \cos \tilde{\alpha})^2}}, \quad (\text{C2})$$

where

$$\sin \gamma = -\frac{\hat{k} \cos \tilde{\alpha}}{\sqrt{(\Delta \hat{k} \sin \tilde{\alpha})^2 + (\hat{k} \cos \tilde{\alpha})^2}} \quad (\text{C3})$$

$$= \begin{cases} -\frac{\cos \tilde{\alpha}}{\sqrt{\hat{\sigma}^2 \sin^2 \tilde{\alpha} + \cos^2 \tilde{\alpha}}}, & \hat{s} = \hat{k}, \\ \frac{\cos \tilde{\alpha}}{\sqrt{\hat{\sigma}^2 \sin^2 \tilde{\alpha} + \cos^2 \tilde{\alpha}}}, & \hat{s} = -\hat{k}, \\ -\frac{\hat{\sigma} \cos \tilde{\alpha}}{\sqrt{\sin^2 \tilde{\alpha} + \hat{\sigma}^2 \cos^2 \tilde{\alpha}}}, & \hat{s} = \Delta \hat{k}, \\ \frac{\hat{\sigma} \cos \tilde{\alpha}}{\sqrt{\sin^2 \tilde{\alpha} + \hat{\sigma}^2 \cos^2 \tilde{\alpha}}}, & \hat{s} = -\Delta \hat{k}, \end{cases}$$

$$\cos \gamma = \frac{\Delta \hat{k} \sin \tilde{\alpha}}{\sqrt{(\Delta \hat{k} \sin \tilde{\alpha})^2 + (\hat{k} \cos \tilde{\alpha})^2}} = \begin{cases} \frac{\hat{\sigma} \sin \tilde{\alpha}}{\sqrt{\hat{\sigma}^2 \sin^2 \tilde{\alpha} + \cos^2 \tilde{\alpha}}}, & \hat{s} = \hat{k}, \\ -\frac{\hat{\sigma} \sin \tilde{\alpha}}{\sqrt{\hat{\sigma}^2 \sin^2 \tilde{\alpha} + \cos^2 \tilde{\alpha}}}, & \hat{s} = -\hat{k}, \\ \frac{\sin \tilde{\alpha}}{\sqrt{\sin^2 \tilde{\alpha} + \hat{\sigma}^2 \cos^2 \tilde{\alpha}}}, & \hat{s} = \Delta \hat{k}, \\ -\frac{\sin \tilde{\alpha}}{\sqrt{\sin^2 \tilde{\alpha} + \hat{\sigma}^2 \cos^2 \tilde{\alpha}}}, & \hat{s} = -\Delta \hat{k}. \end{cases} \quad (\text{C4})$$

Equation (C2) is resolvable when the coupling coefficients  $\hat{k}$  and  $\Delta \hat{k}$  satisfy the necessary condition:

$$4\hat{k}^2 \cos^2 \tilde{\alpha} + 4\Delta \hat{k}^2 \sin^2 \tilde{\alpha} - (\Omega - \omega_2)^2 > 0, \quad (\text{C5})$$

and the stationary solution  $\beta(t) = \hat{\beta}$  is stable when the derivative  $\partial/\partial \beta$  of the right-hand side of Eq. (C1) is negative, which requires

$$(\hat{k} + \Delta \hat{k}) \cos(\tilde{\alpha} + \hat{\beta}) + (\hat{k} - \Delta \hat{k}) \cos(\tilde{\alpha} - \hat{\beta}) > 0. \quad (\text{C6})$$

Equation (C2) has two solutions, but only one of them satisfies the inequality (C6):

$$\hat{\beta} = Q - \gamma, \quad (\text{C7})$$

where  $\gamma$  is given by Eqs. (C4) and (C3), and

$$Q = -\arccos \frac{\Omega - \omega_2}{2\sqrt{(\Delta \hat{k} \sin \tilde{\alpha})^2 + (\hat{k} \cos \tilde{\alpha})^2}} = \begin{cases} -\arccos \left( \frac{\Omega - \omega_2}{2\sqrt{(\hat{\sigma} \sin \tilde{\alpha})^2 + \cos^2 \tilde{\alpha}}} \right), & \hat{s} = |\hat{k}|, \\ -\arccos \left( \frac{\Omega - \omega_2}{2\sqrt{(\sin \tilde{\alpha})^2 + (\hat{\sigma} \cos \tilde{\alpha})^2}} \right), & \hat{s} = |\Delta \hat{k}|. \end{cases} \quad (\text{C8})$$

The above equation means that  $\cos Q$  decays with coupling strength  $\hat{s}$  as  $1/\hat{s}$  excepting the specific case  $\hat{\omega}_2 = \Omega$  where  $\cos Q = 0$ . It follows from Eqs. (C2)–(C8) that the stationary solutions  $\hat{\beta}$  reconstructed for  $\hat{s} = |\hat{k}|$  and  $\hat{s} = |\Delta \hat{k}|$  are equal in a particular case of self-consistent inverse problem with  $\tilde{\alpha} = \pm \pi/4 + \pi n$  and different otherwise.

#### 2. Theoretical order parameter

Taking coupling coefficients  $\hat{k}$  and  $\Delta \hat{k}$  and the reconstructed phase difference  $\hat{\beta}$  we can use Eq. (5) to estimate the order parameter. However, this estimation is purely theoretical, because it assumes that our reconstruction is exact  $\alpha(t) = \tilde{\alpha}$  and the phase locking is reached  $\beta(t) = \hat{\beta}$ . The

theoretical order parameter is then

$$r_{\text{theor}} = \begin{cases} \sqrt{\cos^2 \tilde{\alpha} + \hat{\sigma}^2 \sin^2 \tilde{\alpha} - \frac{(\Omega - \omega_2)^2}{4\hat{s}^2}}, & \hat{s} = |\hat{k}|, \\ \sqrt{\hat{\sigma}^2 \cos^2 \tilde{\alpha} + \sin^2 \tilde{\alpha} - \frac{(\Omega - \omega_2)^2}{4\hat{s}^2}}, & \hat{s} = |\Delta\hat{k}|, \end{cases} \quad (\text{C9})$$

where  $\hat{s}$  and  $\hat{\sigma}$  denote, respectively, the strength and asymmetry of the coupling used in the reconstruction ( $\hat{k}$ ,  $\Delta\hat{k}$ ). In the specific case  $\hat{\omega}_2 = \Omega$  the theoretical order parameter does not depend on the coupling strength.

### 3. Reconstruction of natural frequencies

The phase differences  $\tilde{\alpha}$  and  $\tilde{\beta}$  are the stationary solution of Eq. (A6), then the phase difference  $\Delta\hat{\omega}$  satisfies the following equation:

$$\Delta\hat{\omega} = \hat{k} \sin \tilde{\alpha} \cos \tilde{\beta} + \Delta\hat{k} \sin \tilde{\beta} \cos \tilde{\alpha}. \quad (\text{C10})$$

Now we can substitute  $\tilde{\beta}$  in the first equation of Eq. (A6) and express  $\Delta\hat{\omega}$  through  $\tilde{\alpha}$ :

$$\Delta\hat{\omega} = \begin{cases} \frac{\hat{\sigma}(\Omega - \omega_2) + \hat{s}(1 - \hat{\sigma}^2)r_{\text{theor}} \sin 2\tilde{\alpha}}{2(\hat{\sigma}^2 \sin^2 \tilde{\alpha} + \cos^2 \tilde{\alpha})}, & \hat{s} = |\hat{k}|, \\ \frac{\hat{\sigma}(\Omega - \omega_2) - \hat{s}(1 - \hat{\sigma}^2)r_{\text{theor}} \sin 2\tilde{\alpha}}{2(\sin^2 \tilde{\alpha} + \hat{\sigma}^2 \cos^2 \tilde{\alpha})}, & \hat{s} = |\Delta\hat{k}|. \end{cases} \quad (\text{C11})$$

We reconstruct natural frequencies  $\omega_1$  and  $\omega_3$  as

$$\hat{\omega}_1 = \frac{3}{2}\Omega - \frac{\omega_2}{2} + \Delta\hat{\omega}, \quad \hat{\omega}_3 = \frac{3}{2}\Omega - \frac{\omega_2}{2} - \Delta\hat{\omega}. \quad (\text{C12})$$

When the original coupling coefficients are used in the reconstruction,  $\hat{k} = \tilde{k}$  and  $\Delta\hat{k} = \Delta\tilde{k}$ , the unknown natural frequencies are reconstructed exactly  $\hat{\omega}_1 = \tilde{\omega}_1$  and  $\hat{\omega}_3 = \tilde{\omega}_3$ . When the true coupling is not known we can sometimes reconstruct the right sign of  $\Delta\omega$ , rightly distinguishing the quick and the slow oscillator. Although such reconstruction does not quantify natural frequencies it provides a qualitative knowledge about their order which is important in some applications (see Sec. II B 3).

*Theorem 1.* Let  $\tilde{\alpha}$  be a phase difference of a synchronized Kuramoto chain with three oscillators with natural frequencies  $\tilde{\omega}_i$ , the coupling coefficients  $\tilde{k}$ ,  $\Delta\tilde{k}$ , and the coupling asymmetry  $\tilde{\sigma}$ . Let  $\Delta\hat{\omega}$  be the reconstruction of  $\Delta\omega$  performed with the coupling coefficients  $\hat{k}$ ,  $\Delta\hat{k}$  and the coupling asymmetry  $\hat{\sigma}$  for the known phase difference  $\tilde{\alpha}$  and the frequencies  $\Omega$  and  $\omega_2$ . If the following inequality holds for two pairs  $(\Delta\tilde{\omega}, \tilde{\sigma})$  and  $(\Delta\hat{\omega}, \hat{\sigma})$ ,

$$|\Delta\omega| > \begin{cases} \frac{|\sigma(\Omega - \omega_2)|}{2(\sigma^2 \sin^2 \tilde{\alpha} + \cos^2 \tilde{\alpha})}, & s = |\tilde{k}|, \\ \frac{|\sigma(\Omega - \omega_2)|}{2(\sin^2 \tilde{\alpha} + \sigma^2 \cos^2 \tilde{\alpha})}, & s = |\Delta\tilde{k}|, \end{cases} \quad (\text{C13})$$

then  $\Delta\hat{\omega}$  and  $\Delta\tilde{\omega}$  have the same signs.

*Proof.* In the particular case  $\omega_2 = \Omega$  Eq. (C13) is always satisfied, the first term of the right-hand side of Eq. (C11) is zero and the right hand side simplified to its second term. The signs of both  $\Delta\hat{\omega}$  and  $\Delta\tilde{\omega}$  are similarly determined by the sign of  $\sin 2\tilde{\alpha} = \sin(\theta_1 - \theta_3)$ , which is known. Thus, the reconstructed sign of  $\Delta\hat{\omega}$  always coincides with the true sign of  $\Delta\tilde{\omega}$  if the reconstruction is self-consistent.

To have similar relationship between the sign of  $\Delta\omega$  and  $\sin 2\tilde{\alpha}$  in general case, one need both differences between natural frequencies  $\Delta\tilde{\omega}$  and  $\Delta\hat{\omega}$  to be greater than the first

term of the right hand side of Eq. (C11), which is required by the condition (C13). ■

Let us consider the inverse problem described in Sec. II B applied to the stable phase locked state of the Kuramoto chain with three oscillators with constant phase difference of the edge oscillators  $\tilde{\alpha} = (\tilde{\theta}_1 - \tilde{\theta}_3)/2$  and the mean frequency  $\Omega$ . Then we define the reconstruction performed for coupling coefficients  $\hat{s}$ ,  $\hat{\sigma}$  (or  $\hat{k}$ ,  $\Delta\hat{k}$ ) and natural frequency  $\hat{\omega}_2$  to be self-consistent if a Kuramoto chain with the reconstructed phase differences  $\hat{\omega}_i$  and coupling coefficients  $\hat{s}$ ,  $\hat{\sigma}$  is synchronized to the same mean frequency  $\Omega$  and phase difference between edge oscillators  $\hat{\alpha} = \tilde{\alpha}$ . This definition of self-consistence may be useful when natural frequencies are constant and considered time span is infinite. Even small and smooth variation of natural frequencies make it impossible to reconstruct their dynamics on infinite time span and the reconstructed phase difference between the edge oscillators on a finite time interval will be always different from the original one. Therefore, we imply that the reconstruction is self-consistent when  $\alpha = \tilde{\alpha}$ ,  $\beta = \tilde{\beta}$  is a stable stationary solution of Eq. (C1) with  $\Delta\omega = \Delta\hat{\omega}$ ,  $s = \hat{s}$  and  $\sigma = \hat{\sigma}$ . Thus, correctness of the reconstruction requires the eigenvalues of the Jacobian of Eq. (A6) to be negative. To provide negative eigen values two conditions must be fulfilled: first is given by the the Eq. (C6), and the second is

$$(\hat{k} + \Delta\hat{k})(\hat{k} - \Delta\hat{k}) \cos(\tilde{\alpha} + \tilde{\beta}) \cos(\tilde{\alpha} - \tilde{\beta}) > 0. \quad (\text{C14})$$

To satisfy both (C6) and (C14) the two terms must be positive:

$$\begin{aligned} F^+ &= (\hat{k} + \Delta\hat{k}) \cos(\tilde{\alpha} + \tilde{\beta}) > 0 \quad \text{and} \\ F^- &= (\hat{k} - \Delta\hat{k}) \cos(\tilde{\alpha} - \tilde{\beta}) > 0. \end{aligned} \quad (\text{C15})$$

The following theorem proves that solution of the inverse problem described in Sec. II B is correct when the coupling is strong enough.

*Theorem 2.* Let  $\tilde{\alpha} = \tilde{\theta}/2 \in [-\pi/2, \pi/2]$  be the observed phase difference,  $\hat{k}$  and  $\Delta\hat{k}$  be the coupling coefficients of the reconstruction. Let also that the coupling of the reconstruction be strong enough (there is  $s_0$  such that  $|\hat{s}| > s_0$ ). Then the reconstruction is self-consistent for  $|2\tilde{\alpha}| < \pi/2$  if  $\hat{s} = |\hat{k}|$ . The reconstruction is self-consistent for  $|2\tilde{\alpha}| > \pi/2$  if  $\hat{s} = |\Delta\hat{k}|$ .

*Proof.* Substituting  $\tilde{\beta}$  from Eqs. (C7) and (C8) to the Eq. (C15) after simple transformations we express  $F^+$  and  $F^-$  as follows:

$$\begin{aligned} F^+ &= \begin{cases} \frac{-(1 - \hat{\sigma}^2)(\Omega - \omega_2) \sin 2\tilde{\alpha} + 4\hat{s}r_{\text{theor}}(\hat{\sigma} + 1)(\hat{\sigma} \sin^2 \tilde{\alpha} + \cos^2 \tilde{\alpha})}{4(\hat{\sigma}^2 \sin^2 \tilde{\alpha} + \cos^2 \tilde{\alpha})}, & \hat{s} = |\hat{k}|, \\ \frac{(1 - \hat{\sigma}^2)(\Omega - \omega_2) \sin 2\tilde{\alpha} + 4\hat{s}r_{\text{theor}}(\hat{\sigma} + 1)(\sin^2 \tilde{\alpha} + \hat{\sigma} \cos^2 \tilde{\alpha})}{4(\sin^2 \tilde{\alpha} + \hat{\sigma}^2 \cos^2 \tilde{\alpha})}, & \hat{s} = |\Delta\hat{k}|, \end{cases} \\ F^- &= \begin{cases} \frac{(1 - \hat{\sigma}^2)(\Omega - \omega_2) \sin 2\tilde{\alpha} + 4\hat{s}r_{\text{theor}}(1 - \hat{\sigma})(\cos^2 \tilde{\alpha} - \hat{\sigma} \sin^2 \tilde{\alpha})}{4(\hat{\sigma}^2 \sin^2 \tilde{\alpha} + \cos^2 \tilde{\alpha})}, & \hat{s} = |\hat{k}|, \\ \frac{-(1 - \hat{\sigma}^2)(\Omega - \omega_2) \sin 2\tilde{\alpha} + 4\hat{s}r_{\text{theor}}(1 - \hat{\sigma})(\sin^2 \tilde{\alpha} - \hat{\sigma} \cos^2 \tilde{\alpha})}{4(\sin^2 \tilde{\alpha} + \hat{\sigma}^2 \cos^2 \tilde{\alpha})}, & \hat{s} = |\Delta\hat{k}|. \end{cases} \end{aligned} \quad (\text{C16})$$

When the coupling is strong enough  $\hat{s} > s_0$ , the second term in the denominator dominates the first one. Thus, the self consistent reconstruction requires the second term in the denominators of Eq. (C16) to be positive for all  $\tilde{\sigma}$ . The sign of the second term in Eq. (C16) is governed for  $\hat{s} = |\hat{k}|$  by the sum

$$S = \cos^2 \tilde{\alpha} \pm \hat{\sigma} \sin^2 \tilde{\alpha}, \quad \hat{s} = |\hat{k}|, \quad (\text{C17})$$

and for  $\hat{s} = |\Delta\hat{k}|$  it is governed by the sum

$$S = \sin^2 \tilde{\alpha} \pm \hat{\sigma} \cos^2 \tilde{\alpha}, \quad \hat{s} = |\Delta\hat{k}|. \quad (\text{C18})$$

$S$  in Eq. (C17) is positive for all  $\hat{\sigma}$  only when  $\cos^2 \tilde{\alpha} > \sin^2 \tilde{\alpha}$ , which means  $|2\tilde{\alpha}| < \pi/2$ . Similarly,  $S$  in Eq. (C17) is positive for all  $\hat{\sigma}$  only when  $\cos^2 \tilde{\alpha} < \sin^2 \tilde{\alpha}$ , which means  $|2\tilde{\alpha}| > \pi/2$ . If we consider  $|2\tilde{\alpha}| < \pi/2$  then the reconstruction performed for  $\hat{s} = |\hat{k}|$  gives  $S > 0$  for any  $\hat{\sigma}$ . Then for large enough coupling strength  $\hat{s} > s_0$ , both  $F^+$  and  $F^-$  are positive, ensuring the self-consistent reconstruction. On the contrary, the reconstruction performed for  $\hat{s} = \Delta\hat{k}$  gives negative  $S$  from Eq. (C18), and therefore for any  $\hat{\sigma}$  there exist large enough coupling strength  $\hat{s}$  that makes  $F^+$  or  $F^-$  negative. Therefore, such reconstruction is not self-consistent.

Similar reasoning is applied for  $|2\tilde{\alpha}| > \pi/2$ .

Now let us take  $\hat{s} = |\hat{k}|$  for  $|2\tilde{\alpha}| < \pi/2$  ( $\hat{s} = |\Delta\hat{k}|$  for  $|2\tilde{\alpha}| > \pi/2$ ) and express the necessary coupling strength  $s_0$  required for the domination of the second term in Eq. (C16) for all  $\hat{\sigma}$ . Substituting  $r_{\text{theor}}$  from Eq. (C9) we get from the equation on  $F^+$  for given  $\hat{\sigma}$ :

$$\hat{s}^2 > \begin{cases} \frac{(\Omega - \omega_2)^2}{4(\cos^2 \tilde{\alpha} + \hat{\sigma}^2 \sin^2 \tilde{\alpha})} \left[ 1 + \left( \frac{(1 - \hat{\sigma}) \sin 2\tilde{\alpha}}{2(\hat{\sigma} \sin^2 \tilde{\alpha} + \cos^2 \tilde{\alpha})} \right)^2 \right], & \hat{s} = |\hat{k}|, \\ \frac{(\Omega - \omega_2)^2}{4(\hat{\sigma}^2 \cos^2 \tilde{\alpha} + \sin^2 \tilde{\alpha})} \left[ 1 + \left( \frac{(1 - \hat{\sigma}) \sin 2\tilde{\alpha}}{2(\sin^2 \tilde{\alpha} + \hat{\sigma} \cos^2 \tilde{\alpha})} \right)^2 \right], & \hat{s} = |\Delta\hat{k}|. \end{cases} \quad (\text{C19})$$

Similarly, we get from equation on  $F^-$  for given  $\hat{\sigma}$ :

$$\hat{s}^2 > \begin{cases} \frac{(\Omega - \omega_2)^2}{4(\cos^2 \tilde{\alpha} + \hat{\sigma}^2 \sin^2 \tilde{\alpha})} \left[ 1 + \left( \frac{(1 + \hat{\sigma}) \sin 2\tilde{\alpha}}{2(\hat{\sigma} \sin^2 \tilde{\alpha} - \cos^2 \tilde{\alpha})} \right)^2 \right], & \hat{s} = |\hat{k}|, \\ \frac{(\Omega - \omega_2)^2}{4(\hat{\sigma}^2 \cos^2 \tilde{\alpha} + \sin^2 \tilde{\alpha})} \left[ 1 + \left( \frac{(1 + \hat{\sigma}) \sin 2\tilde{\alpha}}{2(\sin^2 \tilde{\alpha} - \hat{\sigma} \cos^2 \tilde{\alpha})} \right)^2 \right], & \hat{s} = |\Delta\hat{k}|. \end{cases} \quad (\text{C20})$$

To get one boundary  $s_0$  we take maximum of the right-hand side of Eq. (C19) and (C20) by  $\hat{\sigma} \in (-1, 1)$  and then take maximum of both values. The right-hand side of Eqs. (C19) and (C20) is a product of two terms. The first term is maximal when  $\hat{\sigma} = 0$ . The second term in Eq. (C19) has negative derivative by  $\hat{\sigma}$  and therefore reaches its maximum when

$\hat{\sigma} = -1$ . In Eq. (C20) the second term has positive derivative by  $\hat{\sigma}$  and reaches its maximum when  $\hat{\sigma} = 1$ . Taking maxima of both terms after simplification we get the estimate of  $s_0$ :

$$s_0^2 = \begin{cases} \frac{(\Omega - \omega_2)^2}{4 \cos^2 \tilde{\alpha}} \left( 1 + \frac{\sin^2 2\tilde{\alpha}}{\cos^2 2\tilde{\alpha}} \right), & \hat{s} = |\hat{k}|, \\ \frac{(\Omega - \omega_2)^2}{4 \sin^2 \tilde{\alpha}} \left( 1 + \frac{\sin^2 2\tilde{\alpha}}{\cos^2 2\tilde{\alpha}} \right), & \hat{s} = |\Delta\hat{k}|. \end{cases} \quad (\text{C21})$$

When  $\hat{s} > s_0$  the reconstruction is self-consistent for all  $\hat{\sigma}$ . ■

In the specific case  $\hat{\omega}_2 = \Omega$  the boundary  $s_0 = 0$  and any reconstruction appears to be self-consistent for all  $\hat{s}$ .

#### APPENDIX D: RECONSTRUCTED ASYMMETRY OF THE ORDER PARAMETER VERSUS COUPLING STRENGTH OF THE RECONSTRUCTION

When the reconstruction is not exact [ $\alpha(t) \neq \tilde{\alpha}$ ] the reconstructed order parameter is different from the theoretical value obtained in section C 2 ( $\hat{r} \neq r_{\text{theor}}$ ) and therefore the reconstructed asymmetry of the order parameter appears to be nonzero  $\hat{A} \neq 0$ . In Sec. II B we show numerically that  $\hat{A}$  always decay with the coupling strength  $\hat{s}$  used in the reconstruction. Let us now prove analytically that for  $\omega_2 \neq \Omega$  its decay cannot be slower than  $1/\hat{s}$ .

*Proof.* The order parameter is given by Eq. (5) where  $\beta = \hat{\beta}$  and  $\alpha = \alpha(\hat{\sigma}) \neq \tilde{\alpha}$ :

$$r = \begin{cases} \cos \alpha \cos \hat{\beta} - \hat{\sigma} \sin \alpha \sin \hat{\beta}, & \hat{s} = |\hat{k}|, \\ \hat{\sigma} \cos \alpha \cos \hat{\beta} - \sin \alpha \sin \hat{\beta}, & \hat{s} = |\Delta\hat{k}|. \end{cases} \quad (\text{D1})$$

The phase difference  $\alpha$  depends on  $\hat{\sigma}$  and may be represent it in the symmetrical form:

$$\alpha(\hat{\sigma}) = \tilde{\alpha} + \Delta\alpha, \quad \alpha(-\hat{\sigma}) = \tilde{\alpha} - \Delta\alpha, \quad (\text{D2})$$

where

$$\tilde{\alpha} = \frac{\alpha(\hat{\sigma}) + \alpha(-\hat{\sigma})}{2}, \quad \Delta\alpha = \frac{\alpha(\hat{\sigma}) - \alpha(-\hat{\sigma})}{2}. \quad (\text{D3})$$

We substitute  $\hat{\beta} = Q - \gamma$  in Eq. (D1) and get

$$r_{\text{rec}}(\hat{\sigma}) = \begin{cases} \cos(\tilde{\alpha} + \Delta\alpha) \cos(Q - \gamma) - \hat{\sigma} \sin(\tilde{\alpha} + \Delta\alpha) \sin(Q - \gamma), & \hat{s} = |\hat{k}|, \\ \hat{\sigma} \cos(\tilde{\alpha} + \Delta\alpha) \cos(Q - \gamma) - \sin(\tilde{\alpha} + \Delta\alpha) \sin(Q - \gamma), & \hat{s} = |\Delta\hat{k}|, \end{cases} \quad (\text{D4})$$

$$r_{\text{rec}}(-\hat{\sigma}) = \begin{cases} \cos(\tilde{\alpha} - \Delta\alpha) \cos(Q - \gamma) + \hat{\sigma} \sin(\tilde{\alpha} - \Delta\alpha) \sin(Q - \gamma), & \hat{s} = |\hat{k}|, \\ -\hat{\sigma} \cos(\tilde{\alpha} - \Delta\alpha) \cos(Q - \gamma) - \sin(\tilde{\alpha} - \Delta\alpha) \sin(Q - \gamma), & \hat{s} = |\Delta\hat{k}|. \end{cases} \quad (\text{D5})$$

Now we take into account that  $\gamma$  depends on the sign of  $\sigma$  in agreement with Eqs. (C3) and (C4) and  $Q$  does not. We substitute relevant  $\gamma$  in Eq. (D4):

$$r_{\text{rec}}(\hat{\sigma}) = \begin{cases} \frac{\cos(\tilde{\alpha} + \Delta\alpha)(\hat{\sigma} \cos Q \sin \tilde{\alpha} - \sin Q \cos \tilde{\alpha}) - \hat{\sigma} \sin(\tilde{\alpha} + \Delta\alpha)(\hat{\sigma} \sin Q \sin \tilde{\alpha} + \cos Q \cos \tilde{\alpha})}{\sqrt{\hat{\sigma}^2 \sin^2 \tilde{\alpha} + \cos^2 \tilde{\alpha}}}, & \hat{s} = \hat{k}, \\ \frac{\cos(\tilde{\alpha} + \Delta\alpha)(-\hat{\sigma} \cos Q \sin \tilde{\alpha} + \sin Q \cos \tilde{\alpha}) + \hat{\sigma} \sin(\tilde{\alpha} + \Delta\alpha)(\hat{\sigma} \sin Q \sin \tilde{\alpha} + \cos Q \cos \tilde{\alpha})}{\sqrt{\hat{\sigma}^2 \sin^2 \tilde{\alpha} + \cos^2 \tilde{\alpha}}}, & \hat{s} = -\hat{k}, \\ \frac{\hat{\sigma} \cos(\tilde{\alpha} + \Delta\alpha)(\cos Q \sin \tilde{\alpha} - \hat{\sigma} \sin Q \cos \tilde{\alpha}) - \sin(\tilde{\alpha} + \Delta\alpha)(\sin Q \sin \tilde{\alpha} + \hat{\sigma} \cos Q \cos \tilde{\alpha})}{\sqrt{\hat{\sigma}^2 \sin^2 \tilde{\alpha} + \cos^2 \tilde{\alpha}}}, & \hat{s} = \Delta\hat{k}, \\ \frac{\hat{\sigma} \cos(\tilde{\alpha} + \Delta\alpha)(-\cos Q \sin \tilde{\alpha} + \hat{\sigma} \sin Q \cos \tilde{\alpha}) + \sin(\tilde{\alpha} + \Delta\alpha)(\sin Q \sin \tilde{\alpha} + \hat{\sigma} \cos Q \cos \tilde{\alpha})}{\sqrt{\hat{\sigma}^2 \sin^2 \tilde{\alpha} + \cos^2 \tilde{\alpha}}}, & \hat{s} = -\Delta\hat{k}, \end{cases}$$

$$r_{\text{rec}}(-\hat{\sigma}) = \begin{cases} \frac{-\cos(\bar{\alpha}-\Delta\alpha)(\hat{\sigma}\cos Q\sin\bar{\alpha}+\sin Q\cos\bar{\alpha})+\hat{\sigma}\sin(\bar{\alpha}-\Delta\alpha)(-\hat{\sigma}\sin Q\sin\bar{\alpha}+\cos Q\cos\bar{\alpha})}{\sqrt{\hat{\sigma}^2\sin^2\bar{\alpha}+\cos^2\bar{\alpha}}}, & \hat{s} = \hat{k}, \\ \frac{\cos(\bar{\alpha}-\Delta\alpha)(\hat{\sigma}\cos Q\sin\bar{\alpha}+\sin Q\cos\bar{\alpha})-\hat{\sigma}\sin(\bar{\alpha}-\Delta\alpha)(-\hat{\sigma}\sin Q\sin\bar{\alpha}+\cos Q\cos\bar{\alpha})}{\sqrt{\hat{\sigma}^2\sin^2\bar{\alpha}+\cos^2\bar{\alpha}}}, & \hat{s} = -\hat{k}, \\ \frac{-\hat{\sigma}\cos(\bar{\alpha}-\Delta\alpha)(\cos Q\sin\bar{\alpha}+\hat{\sigma}\sin Q\cos\bar{\alpha})-\sin(\bar{\alpha}-\Delta\alpha)(\sin Q\sin\bar{\alpha}-\hat{\sigma}\cos Q\cos\bar{\alpha})}{\sqrt{\sin^2\bar{\alpha}+\hat{\sigma}^2\cos^2\bar{\alpha}}}, & \hat{s} = \Delta\hat{k} \\ \frac{\hat{\sigma}\cos(\bar{\alpha}-\Delta\alpha)(\cos Q\sin\bar{\alpha}+\hat{\sigma}\sin Q\cos\bar{\alpha})+\sin(\bar{\alpha}-\Delta\alpha)(\sin Q\sin\bar{\alpha}-\hat{\sigma}\cos Q\cos\bar{\alpha})}{\sqrt{\sin^2\bar{\alpha}+\hat{\sigma}^2\cos^2\bar{\alpha}}}, & \hat{s} = -\Delta\hat{k}. \end{cases} \quad (\text{D6})$$

Asymmetry of the order parameter is then

$$\hat{A} = |r(\hat{\sigma}) - r(-\hat{\sigma})| = \begin{cases} \frac{|2\hat{\sigma}\cos Q\cos\Delta\alpha\sin(\bar{\alpha}-\bar{\alpha})+\sin Q\sin\Delta\alpha[(1-\hat{\sigma}^2)\sin(\bar{\alpha}+\bar{\alpha})-(1+\hat{\sigma}^2)\sin(\bar{\alpha}-\bar{\alpha})]|}{\sqrt{\hat{\sigma}^2\sin^2\bar{\alpha}+\cos^2\bar{\alpha}}}, & \hat{s} = |\hat{k}|, \\ \frac{|2\hat{\sigma}\cos Q\cos\Delta\alpha\sin(\bar{\alpha}-\bar{\alpha})-\sin Q\sin\Delta\alpha[(1-\hat{\sigma}^2)\sin(\bar{\alpha}+\bar{\alpha})+(1+\hat{\sigma}^2)\sin(\bar{\alpha}-\bar{\alpha})]|}{\sqrt{\sin^2\bar{\alpha}+\hat{\sigma}^2\cos^2\bar{\alpha}}}, & \hat{s} = |\Delta\hat{k}|. \end{cases} \quad (\text{D7})$$

Let us study the asymptotic behavior of the asymmetry  $\hat{A}$  with the coupling strength  $\hat{s}$ . Phase differences  $\alpha(\hat{\sigma})$  and  $\alpha(-\hat{\sigma})$  satisfy equation in Eq. (C1) with constant  $\beta = \hat{\beta}(\hat{\sigma})$  and  $\beta = \hat{\beta}(-\hat{\sigma})$  respectively. Therefore,

$$\frac{|\Omega - \hat{\omega}_2|}{2\hat{s}} = \begin{cases} |\sin(Q - \gamma(\hat{\sigma}))\cos(\bar{\alpha} + \Delta\alpha) + \hat{\sigma}\cos(Q - \gamma(\hat{\sigma}))\sin(\bar{\alpha} + \Delta\alpha)|, & \hat{s} = |\hat{k}|, \\ |\hat{\sigma}\sin(Q - \gamma(\hat{\sigma}))\cos(\bar{\alpha} + \Delta\alpha) + \cos(Q - \gamma(\hat{\sigma}))\sin(\bar{\alpha} + \Delta\alpha)|, & \hat{s} = |\Delta\hat{k}|, \end{cases} \quad (\text{D8})$$

and

$$\frac{|\Omega - \hat{\omega}_2|}{2\hat{s}} = \begin{cases} |\sin(Q - \gamma(-\hat{\sigma}))\cos(\bar{\alpha} - \Delta\alpha) - \hat{\sigma}\cos(Q - \gamma(-\hat{\sigma}))\sin(\bar{\alpha} - \Delta\alpha)|, & \hat{s} = |\hat{k}|, \\ |\hat{\sigma}\sin(Q - \gamma(-\hat{\sigma}))\cos(\bar{\alpha} - \Delta\alpha) - \cos(Q - \gamma(-\hat{\sigma}))\sin(\bar{\alpha} - \Delta\alpha)|, & \hat{s} = |\Delta\hat{k}|, \end{cases} \quad (\text{D9})$$

where  $\gamma$  depend on the sign of  $\sigma$  in agreement with Eqs. (C3) and (C4) and  $Q$  does not. Taking the sum of relevant equations in Eqs. (D8) and (D9) and substituting  $\gamma$  we get

$$\frac{|\Omega - \hat{\omega}_2|}{\hat{s}} = \begin{cases} \frac{|2\hat{\sigma}\sin Q\sin\Delta\alpha\cos(\bar{\alpha}-\bar{\alpha})-\cos Q\cos\Delta\alpha((1-\hat{\sigma}^2)\cos(\bar{\alpha}+\bar{\alpha})+(1+\hat{\sigma}^2)\cos(\bar{\alpha}-\bar{\alpha}))|}{\sqrt{\hat{\sigma}^2\sin^2\bar{\alpha}+\cos^2\bar{\alpha}}}, & \hat{s} = |\hat{k}|, \\ \frac{|2\hat{\sigma}\sin Q\sin\Delta\alpha\sin(\bar{\alpha}-\bar{\alpha})+\cos Q\cos\Delta\alpha((1-\hat{\sigma}^2)\cos(\bar{\alpha}+\bar{\alpha})-(1+\hat{\sigma}^2)\cos(\bar{\alpha}-\bar{\alpha}))|}{\sqrt{\hat{\sigma}^2\sin^2\bar{\alpha}+\cos^2\bar{\alpha}}}, & \hat{s} = |\Delta\hat{k}|. \end{cases} \quad (\text{D10})$$

Taking the difference between the equations we get

$$0 = \begin{cases} \frac{2\hat{\sigma}\sin Q\cos\Delta\alpha\sin(\bar{\alpha}-\bar{\alpha})-\cos Q\sin\Delta\alpha[(1-\hat{\sigma}^2)\sin(\bar{\alpha}+\bar{\alpha})-(1+\hat{\sigma}^2)\sin(\bar{\alpha}-\bar{\alpha})]}{\sqrt{\hat{\sigma}^2\sin^2\bar{\alpha}+\cos^2\bar{\alpha}}}, & \hat{s} = |\hat{k}|, \\ \frac{2\hat{\sigma}\sin Q\cos\Delta\alpha\sin(\bar{\alpha}-\bar{\alpha})+\cos Q\sin\Delta\alpha[(1-\hat{\sigma}^2)\sin(\bar{\alpha}+\bar{\alpha})+(1+\hat{\sigma}^2)\sin(\bar{\alpha}-\bar{\alpha})]}{\sqrt{\hat{\sigma}^2\sin^2\bar{\alpha}+\cos^2\bar{\alpha}}}, & \hat{s} = |\Delta\hat{k}|. \end{cases} \quad (\text{D11})$$

It follows from Eq. (C8) that if  $\omega_2 \neq \Omega$ , then  $\cos Q$  decays with the coupling strength  $\hat{s}$  as  $1/\hat{s}$ . It follows from Eq. (D11) that

$$\hat{\sigma}\sin Q\cos\Delta\alpha\sin(\bar{\alpha}-\bar{\alpha}) = \cos Q\sin\Delta\alpha[(1-\hat{\sigma}^2)\sin(\bar{\alpha}+\bar{\alpha})-(1+\hat{\sigma}^2)\sin(\bar{\alpha}-\bar{\alpha})]. \quad (\text{D12})$$

The right-hand side of the above equation decays at least as  $1/\hat{s}$ , therefore the left-hand side must do it as well. We know that  $\sin Q$  does not decay, therefore  $\cos\Delta\alpha\sin(\bar{\alpha}-\bar{\alpha})$  decays at least as  $1/\hat{s}$ . Consequently, the first term in the asymmetry of Eq. (D7) decays at least as  $1/\hat{s}^2$ . Similarly, we obtain from Eq. (D10) that the first term in the right-hand side must decay at least as  $1/\hat{s}$ , which gives us that  $\sin\Delta\alpha\cos(\bar{\alpha}-\bar{\alpha})$  decays at least as  $1/\hat{s}$ . Since sine and cosine cannot tend to zero simultaneously, we obtain that either  $\cos\Delta\alpha$  and  $\cos(\bar{\alpha}-\bar{\alpha})$  decays at least as  $1/\hat{s}$  or  $\sin\Delta\alpha$  and  $\sin(\bar{\alpha}-\bar{\alpha})$  decays at least as  $1/\hat{s}$ . The first option contradicts correctness of the reconstruction, leaving us with the second option and  $\sin\Delta\alpha$  decaying at least as  $1/\hat{s}$ . Consequently, the second term in Eq. (D7) decays at least as  $1/\hat{s}$ .

#### APPENDIX E: SOLAR CYCLE PHASE

Taking the mean value of the solar cycle length to be equal  $\Theta = 10.75$  years we use the Fourier transform in a centered

sliding window of the length  $\Theta$  to estimate the continuous solar cycle phases  $\Phi_P(t)$  and  $\Phi_T(t)$  with respect to the mean solar cycle frequency  $\Omega_0 = 2\pi/\Theta$ ,

$$A_f(t) + iB_f(t) = \int_{t-\Theta/2}^{t+\Theta/2} f(\tau)[\cos(\Omega\tau) + i\sin(\Omega\tau)]d\tau, \quad (\text{E1})$$

and determine the phase

$$\Phi_f(t) = -\arctan \frac{A_f(t)}{B_f(t)} \quad (\text{E2})$$

in the interval  $[-\pi/2, \pi/2]$ . To get continuous phase we occasionally add or subtract  $\pi$  to  $\Phi_f(t+1)$  when it performs a strong jump with respect to  $\Phi_F(t)$  requiring  $|\Phi_f(t) - \Phi_f(t+1)| < \pi/2$ .

- [1] Y. Kuramoto, *Lect. Notes Phys.* **39**, 420 (1975).
- [2] J. A. Acebrón, L. L. Bonilla, C. J. P. Vicente, F. Ritort, and R. Spigler, *Rev. Mod. Phys.* **77**, 137 (2005).
- [3] F. Dörfler and F. Bullo, *Automatica* **50**, 1539 (2014).
- [4] F. Rodrigues, T. Peron, P. Ji, and J. Kurths, *Phys. Rep.* **610**, 1 (2016).
- [5] T. Stankovski, in *Physics of Biological Oscillators*, Understanding Complex Systems, edited by A. Stefanovska and P. V. E. McClintock (Springer, Cham, 2021), pp. 175–189.
- [6] F. Alderisio, G. Fiore, and M. di Bernardo, *Phys. Rev. E* **95**, 042302 (2017).
- [7] A. Pikovsky, *Phys. Lett. A* **382**, 147 (2018).
- [8] M. Rosenblum and A. Pikovsky, *Chaos* **28**, 106301 (2018).
- [9] M. J. Panaggio, M.-V. Ciocanel, L. Lazarus, C. M. Topaz, and B. Xu, *Chaos* **29**, 103116 (2019).
- [10] K. Manoj, S. A. Pawar, and R. I. Sujith, *Phys. Rev. E* **103**, 022207 (2021).
- [11] T. Ito, K. Konishi, T. Sano, H. Wakayama, and M. Ogawa, *Phys. Rev. E* **105**, 014201 (2022).
- [12] E. M. Blanter, J.-L. Le Mouél, M. G. Shnirman, and V. Courtillot, *Sol. Phys.* **289**, 4309 (2014).
- [13] E. Blanter, J.-L. Le Mouél, M. Shnirman, and V. Courtillot, *Sol. Phys.* **291**, 1003 (2016).
- [14] E. Blanter, J.-L. Le Mouél, M. Shnirman, and V. Courtillot, *Sol. Phys.* **292**, 54 (2017).
- [15] E. Blanter, J.-L. Le Mouél, M. Shnirman, and V. Courtillot, *Sol. Phys.* **293**, 134 (2018).
- [16] E. Blanter and M. Shnirman, *Sol. Phys.* **296**, 86 (2021).
- [17] A. Choudhuri, M. Schussler, and M. Dikpati, *Astron. Astrophys.* **303**, L29 (1995).
- [18] D. H. Hathaway and L. Upton, *J. Geophys. Res.: Space Phys.* **119**, 3316 (2014).
- [19] R. Chen and J. Zhao, *Astrophys. J.* **849**, 144 (2017).
- [20] D. Hathaway, *Liv. Rev. Solar Phys.* **12**, 4 (2015).
- [21] I. Lopes, D. Passos, N. M., and K. Petrovay, *Space Sci. Rev.* **186**, 535 (2014).
- [22] K. Petrovay, *Liv. Rev. Solar Phys.* **17**, 2 (2020).
- [23] P. Kumar, M. Nagy, A. Lemerle, B. B. Karak, and K. Petrovay, *Astrophys. J.* **909**, 87 (2021).
- [24] A. Savostianov, A. Shapoval, and M. Shnirman, *Commun. Nonlin. Sci. Numer. Simul.* **83**, 105149 (2020).
- [25] A. Savostyanov, A. Shapoval, and M. Shnirman, *Physica D* **401**, 132160 (2020).
- [26] G. Cecchini, R. Cestnik, and A. Pikovsky, *Phys. Rev. E* **103**, 022305 (2021).
- [27] T. Rings, T. Bröhl, and K. Lehnertz, *Sci. Rep.* **12**, 11742 (2022).
- [28] H. Hong and S. H. Strogatz, *Phys. Rev. Lett.* **106**, 054102 (2011).
- [29] S. N. Chowdhury, D. Ghosh, and C. Hens, *Phys. Rev. E* **101**, 022310 (2020).
- [30] K. Kovalenko, X. Dai, K. Alfaro-Bittner, A. M. Raigorodskii, M. Perc, and S. Boccaletti, *Phys. Rev. Lett.* **127**, 258301 (2021).
- [31] H. Hong and S. H. Strogatz, *Phys. Rev. E* **85**, 056210 (2012).
- [32] S. N. Chowdhury, S. Rakshit, J. M. Buldú, D. Ghosh, and C. Hens, *Phys. Rev. E* **103**, 032310 (2021).
- [33] D. M. Abrams and S. H. Strogatz, *Phys. Rev. Lett.* **93**, 174102 (2004).
- [34] F. Parastesh, S. Jafari, H. Azarnoush, Z. Shahriari, Z. Wang, S. Boccaletti, and M. Perc, *Phys. Rep.* **898**, 1 (2021).
- [35] N. Kruk, Y. Maistrenko, and H. Koepl, *Chaos* **30**, 111104 (2020).
- [36] P. Jaros, R. Levchenko, T. Kapitaniak, and Y. Maistrenko, *Chaos* **31**, 103111 (2021).
- [37] P. Jaros, S. Brezetsky, R. Levchenko, D. Dudkowski, T. Kapitaniak, and Y. Maistrenko, *Chaos* **28**, 011103 (2018).
- [38] B. Chen, J. R. Engelbrecht, and R. Mirolo, *Chaos* **29**, 013126 (2019).
- [39] M. Schröder, M. Timme, and D. Witthaut, *Chaos* **27**, 073119 (2017).
- [40] D. H. Zanette, *Europhys. Lett.* **72**, 190 (2005).
- [41] Z. Levnajić, *Phys. Rev. E* **84**, 016231 (2011).
- [42] P. Charbonneau, *Liv. Rev. Solar Phys.* **17**, 4 (2020).
- [43] <https://www.sidc.be/silso/exthemium>.
- [44] A. M. Veronig, S. Jain, T. Podladchikova, W. Pötzi, and F. Clette, *Astron. Astrophys.* **652**, A56 (2021).
- [45] A. Muñoz-Jaramillo, N. Sheeley, J. Zhang, and E. DeLuca, *Astrophys. J.* **753**, 146 (2012).
- [46] [http://www.gaoran.ru/database/esai/yr\\_pfs.txt](http://www.gaoran.ru/database/esai/yr_pfs.txt).
- [47] E. Teichmann and M. Rosenblum, *Chaos* **29**, 093124 (2019).
- [48] H. Sakaguchi and Y. Kuramoto, *Prog. Theor. Phys.* **76**, 576 (1986).
- [49] T. Ichinomiya, *Phys. Rev. E* **70**, 026116 (2004).
- [50] S.-H. Yook and Y. Kim, *Phys. Rev. E* **97**, 042317 (2018).
- [51] J. R. Engelbrecht and R. Mirolo, *Phys. Rev. Res.* **2**, 023057 (2020).